This is a “preproof” accepted article for *Mineralogical Magazine*.

This version may be subject to change during the production process.

10.1180/mgm.2024.100

Contrasting assemblages of secondary minerals after beryl from granitic pegmatites Drahonín IV and Věžná I; evidence for high variability of mineralized fluids in the Rožná-Olší ore field area

Milan NOVÁK[1], Petr GADAS[1], Kamil SOBEK[2], Jiří TOMAN[3]*, Drahoš ŠIKOLA[4]

[1] *Department of Geological Sciences, Faculty of Science, Masaryk University, Kotlářská 2, CZ-611 37 Brno, Czech Republic*

[2] *Department of Material Analysis, Research Centre Řež, Hlavní 130, Husinec-Řež, CZ-250 68*

[3] *Department of Mineralogy and Petrography, Moravian Museum, Zelný trh 6, CZ-659 37 Brno, Czech Republic, email: jtoman@mzm.cz, +420 533435216*

[4] *Diamo, S. E., Branch GEAM, CZ-592 51 Dolní Rožínka, Czech Republic*

** Corresponding author*

Abstract

Mineral assemblages, chemical composition, and Raman spectroscopy of proximal secondary Be-minerals and associated minerals in pseudomorphs after beryl from granitic pegmatites located along the contact of major regional geological units were examined. The pegmatites differ evidently in their position to the ductile to brittle shear zones within the Rožná-Olší ore field (U-deposit). Extensive dissolution of beryl crystals in the beryl-columbite pegmatites Drahonín IV and Věžná I situated within or close to the shear zones were studied in detail, whereas alterations of beryl in the Dolní Rožínka and Kovářová pegmatites located out of the shear zones are minor. Almost total replacement of beryl crystals, up to 40 cm long, from the Drahonín IV pegmatite located in the Olší shear zone generated the following secondary Be-minerals given in their abundance: bavenite-bohseite > bertrandite >> milarite > hydroxylgugiaite. This assemblage also is characterized by the presence of sulphides (pyrite,

galena, sphalerite) and zeolites. Such an extensive process required a massive fluid flow and is very likely related to the pre-uranium quartz-sulphide and carbonate-sulphide mineralizations within the Rožná-Olší ore field. Alterations products resulting from breakdown of beryl in the Věžná I pegmatite accompanying the sequential substages (bertrandite + K-feldspar ± harmotome → epidydimite + K-feldspar → hydroxylgugiatite + K-feldspar) locally show crosscutting textures. These assemblages were generated by postmagmatic residual fluids (early assemblage bertrandite + K-feldspar) as well as fluids related to a retrograde stage of metamorphism, compositionally contrasting host serpentinite and perhaps also hydrothermal processes associated with the Olší shear zone. The pegmatites Dolní Rožínka and Kovářová located out of the shear zones exhibit only a low degree of alteration and its different textural and paragenetic development. Highly variable assemblages of secondary minerals after beryl are outstanding mineral indicators of hydrothermal overprint in granitic pegmatites during a variety of subsolidus processes.
Keywords: beryl, secondary Be-minerals, granitic pegmatites, internal hydrothermal fluids, external hydrothermal fluids

1. Introduction

Beryllium minerals are typical minor to rare accessory minerals in a large variety of rocks. They mostly occur in granitic pegmatites of almost all classes/types defined by Černý and Ercit (2005) from abyssal (anatectic) pegmatites (e.g., Grew *et al.*, 1998; Grew, 2002; Cempírek *et al.*, 2010) to rare-element pegmatites and miarolitic pegmatites of LCT (Lithium-Tantalum-Cesium) and NYF (Niobium-Yttrium-Fluorine) families (e.g., Černý, 2002; London, 2008; Černý *et al.*, 2012) or Group A (Wise *et al.*, 2022) where beryl is typically by far the most abundant primary Be-mineral. Beryl from granitic pegmatites frequently underwent hydrothermal alteration at different stages of their subsolidus evolution (e.g., Černý, 2002; London, 2008, 2014; Wang *et al.*, 2009; Novák and Filip, 2010; Uher *et al.*, 2010, 2022; Novák *et al.*, 2023a). They were facilitated by residual pegmatite fluids (e.g., Palinkaš *et al*., 2014; Zachař *et al.*, 2020; Novák *et al*., 2023a) and/or by external fluids derived from host rock after solidification of pegmatite melt in different stages of subsolidus evolution of a pegmatite body (e.g., Novák *et al*., 2017, 2023a; Zachař *et al*., 2020; Čopjaková *et al*., 2021; Chládek *et al*., 2021, 2024). However, the timing of the residual fluid exsolution from pegmatite melt is still a matter of debate (e.g., Burnham and Nekvasil, 1986; Veksler and Thomas, 2002; London 2008, Thomas *et al.*, 2009; Thomas and Davidson, 2012) as well

as the timing and sources of external fluids (e.g., Martin and De Vito, 2014; Palinkaš *et al*., 2014; Novák *et al*., 2012, 2017, 2023a; Pieczka *et al*., 2019). Because externally imposed chemical potentials govern stability of Be-minerals along with *PT*-conditions (e.g., Barton, 1986; Barton and Young, 2002; Grew, 2002), primary and secondary Be-minerals, as well as their mineral assemblages, serve as very sensitive geochemical and petrological mineral indicators (e.g., Burt, 1978; Hsu, 1983; Wood, 1992; Markl and Schumacher, 1997; Černý, 2002; Franz and Morteani, 2002; London and Evensen, 2002; Wang *et al*., 2009; Novák and Filip, 2010; Uher *et al*., 2010, 2022; Palinkaš *et al*., 2014; Wang and Li, 2020; Novák *et al*., 2023a).

Four small beryl-bearing granitic pegmatites (Drahonín IV, Věžná I, Dolní Rožínka, Kovářová) with contrasting assemblages of secondary Be-minerals occur along the eastern border of the Strážek Unit, Moldanubian Zone. Due to their distinct position along the shear zones in the Rožná-Olší ore field (U-deposits) they appeared to be very suitable objects for investigation of hydrothermal processes proceeding along tectonically active major regional geological units where a variety of hydrothermal mineralizations is developed chiefly at the Rožná-Olší ore field (Kříbek *et al*., 2009; Novák *et al*., 2023b). We examined mineral assemblages and chemical composition of proximal secondary Be-minerals in pseudomorphs after beryl at the pegmatites with respect to the ductile to brittle shear zones Rožná and Olší. Subsolidus hydrothermal processes, including extensive dissolution of beryl crystals at the Drahonín IV and Věžná I pegmatites, were studied in detail to reveal PT conditions of these alteration processes as well as the composition of fluids, their potential sources and the role of fine-scale brittle tectonics in this region.

2. Geological setting

The Moldanubian Zone represents a crustal (and upper mantle) tectonic collage assembled during the Variscan orogeny (~370–300 Ma). Two main lithotectonic units with distinct lithologies have been recognized: (i) Drosendorf Unit, structurally divided on the lowermost Monotonous Group overlain by the Varied Group, overlain by (ii) the structurally highest high-grade Gföhl Unit (e.g., Guy *et al*., 2011; Schulmann *et al*., 2014 and references therein). The metamorphic rocks experienced a polyphase metamorphic evolution; an HT-HP event in upper amphibolite to granulite facies at $T_{max.}$ ~900-1000 °C and $P_{max.}$ = 1.6-2.0 GPa and dated at ~345-340 Ma (Kotková, 2007) was overprinted during a rapid decompression by an HT-MP event at T < ~700 °C and P ~0.4-0.6 GPa (e.g., Tajčmanová *et al*., 2006; Pertoldová *et al*., 2009, 2010; Štípská *et al*., 2016).

The easternmost part of the Moldanubian Zone, the Strážek Unit (Fig. 1), is built of the Gföhl Unit and Varied Group. The NNW–SSE- to NNE–SSW-striking foliation in rocks from the eastern part of the Strážek Unit is interpreted as a result of E–W compression at lower crustal levels (Tajčmanová *et al*., 2006; Verner *et al*., 2009). Longitudinal N–S to NNW–SSE-striking ductile shear zones (Rožná and Olší shear zones; Fig. 2) dip WSW at an angle of 70–90° and strike parallel to the tectonic contact between the Strážek Unit and the Svratka Crystalline Unit. Along with bodies of (ultra)potassic syenites (e.g., Drahonín body) related to the Třebíč Pluton (Leichmann *et al*., 2017; Janoušek *et al*., 2020; Kubeš *et al*., 2022) and tourmaline-bearing leucogranites (Jiang *et al*., 2003; Buriánek and Novák, 2007; Buriánek *et al*., 2016), abundant rare-element granitic pegmatites (e.g., Rožná, Dobrá Voda, Věžná I, II, Drahonín III, IV, Rečice, Pikárec, Strážek, Dolní Bory - Hatě, Cyrilov; Novák and Cempírek, 2010; Novák *et al*., 2015a), some of them dated at 337-332 Ma (Novák *et al*., 1998; Melleton *et al*., 2012, Ackerman *et al*., 2017) occur in this area. They intruded various metamorphic rocks of the Strážek Unit at a shallow crust level of P < ~0.2-0.3 GPa (Ackermann *et al*., 2007; Novák *et al*., 2013).

3. Internal structure and mineral assemblages of the pegmatites

The examined beryl-bearing granitic pegmatites include the Drahonín IV pegmatite from the U-mine Drahonín in the Rožná-Olší ore field which closed in the late 1960s, and the Věžná I pegmatite situated E of the Olší shear zone (Fig. 2). The Dolní Rožínka pegmatite (Novotný and Cempírek, 2021) located W of the Rožná and Olší shear zones and the Kovářová pegmatite from the adjacent part of Svratka Crystalline Unit located east of the Rožná-Olší shear zone (Přikryl *et al*., 2012, 2014) also were included in this study because they are located outside of the shear zones (Fig. 2). Geological setting, host rocks, and hydrothermal alterations of these pegmatites are presented in Table 1 which illustrates that they have similar size and most exhibit comparable overall primary mineral assemblages and zoned internal structure.

The Drahonín IV pegmatite located very close to the main shaft of the Drahonín U-mine, 3rd level was accessible during active mining in the 1960s (Sojka, 1969). Cross section through the pegmatite dike (Fig. 3) shows an irregular zoned internal structure with up to ~1 m-sized miarolitic pocket lined with large crystals of quartz overgrown by late calcite and pyrite. Comparing the other examined pegmatites, it is situated on or very close to the NNW–SSE striking Olší shear zone, where several hydrothermal mineralizations are developed. They include (i) pre-uranium quartz-sulphide and carbonate-sulphide mineralizations, three

types of uranium mineralization (iia) network disseminated coffinite > uraninite mineralizations, (iib) vein-type ore uraninite > coffinite in calcite veins typically from the upper part of the deposit, and (iic) disseminated coffinite locally accompanied by U-Zr-silicate mineralizations in albititized, desilicified, and commonly porous rocks) and (iii) post-uranium carbonate-quartz-sulphide mineralization (e.g., Kříbek *et al*., 2009) as well as three distinct generations of zeolite and apophyllite mineralizations (Novák *et al*., 2023b).

The Věžná I pegmatite is a steeply dipping NW-striking dike with almost symmetric zoning cutting a serpentinite body (Fig. 4; Černý, 1965; Černý and Povondra, 1966, 1967; Černý *et al*., 1984, 2000; Dosbaba and Novák, 2012; Novák *et al*., 2017; Toman and Novák, 2020). The blocky unit contains large masses of albite, up to several dm in size, locally with minor Be-cordierite, schorl-dravite, beryl, and several accessory minerals (Table 1). Brownish blocky K-feldspar with very rare Cs,Li-rich mineral assemblage (pollucite + elbaite + lepidolite) in the albite-pollucite unit represents the most fractionated but volumetrically negligible Cs,Li-rich unit (Teertstra *et al*., 1995; Toman and Novák, 2018, 2020).

Mineral assemblages of the individual pegmatites are quite similar (Table 1). Occurrences of Al-rich minerals (Ms, Tur, Crd, Grt) as well as common accessory fluor-apatite indicate peraluminous LCT signature (Černý *et al*., 2012) of these pegmatites. The main differences include the degree of fractionation, high in the pegmatites with Li- and Cs-minerals (Dolní Rožínka; Novotný and Cempírek, 2021 and Věžná I; Teertstra *et al*., 1995; Toman and Novák, 2018, 2020), and strong external contamination from host serpentinite in the Věžná I pegmatite (e.g., Dosbaba and Novák, 2012; Novák *et al*., 2017; Čopjaková *et al*., 2021).

4. Beryl and its breakdown products from the Drahonín IV, Věžná I, Dolní Rožínka and Kovářová pegmatites

Beryl, typically the only primary Be-mineral at the studied localities, was found in several distinct textural/paragenetic and compositional types within single pegmatite dikes as at other pegmatites worldwide (e.g., Černý *et al*., 2003; Wang *et al*., 2009; Uher *et al*., 2010, 2022). Consequently, we used the following abbreviations for description purposes to recognize distinct types of primary beryl and secondary recrystallized beryl because it was often recrystallized during early subsolidus processes (e.g., Wang *et al*., 2009; Novák and Filip, 2010; Přikryl *et al*., 2014; Uher *et al*., 2022; Chládek *et al*., 2024). Primary beryl (homogeneous or with coarse oscillatory zoning) is labelled as beryl I, II, III and IV from different textural/paragenetic units generally arranged from the least to the most evolved pegmatite units and there are no relations between these symbols from the individual

pegmatites. Recrystallized secondary beryl, mostly as compositionally heterogeneous veinlets or irregular masses replacing early primary beryl, is marked as beryl IA, IIA etc. This terminology is in general consistent with the nomenclatures of beryl used by Wang *et al*., (2009), Uher *et al*., (2010) and Novotný and Cempírek (2021). Beryl and its breakdown products were already studied and are given in Table 2.

In the Drahonín IV pegmatite**,** large prismatic crystals of beryl with hexagonal shape, up to ~40 cm long and ~15 cm thick, occurred in strongly albitized blocky K-feldspar and they were often almost completely dissolved (Sojka, 1969). Secondary bavenite was described but not examined in detail by this author but was recently studied in detail by Novák *et al*. (2023a) as $Bav_{56-40}Boh_{60-44}$. Relics of homogeneous primary beryl II are more common. Toman and Novák (2020) recognized three distinct paragenetic and textural types of primary beryl at the Věžná I pegmatite; beryl I as rare pale yellowish to greenish subhedral grains, up to 5 mm in size, associated with black tourmaline and albite; the most abundant greyish to pale greenish beryl II as large subhedral to euhedral crystals, up to 20 cm long, in the intermediate blocky unit and albite (Novák *et al*., 1991; Toman and, Novák 2020); very rare equant anhedral grains of colorless Cs-enriched beryl III, up to 8 mm in size, in albite close to brownish blocky K-feldspar and Cs,Li-rich mineralization (Toman and Novák, 2018, 2020). Columnar crystals of beryl II are locally recrystallized to beryl IIA (veinlets of Cs-enriched beryl) and frequently replaced by a fine-grained aggregate of secondary phases (Černý, 1963, 1965, 1968; Novák *et al*., 1991) whereas rare small grains of beryl I and beryl III were not altered. Novák *et al*. (1991) described an almost complete pseudomorph after beryl II consisting of the assemblage bertrandite + epidydimite + K-feldspar + muscovite (Table 2).

5. Methods and samples

Sampling

The examined samples of beryl and other associated minerals from the Drahonín IV pegmatite were collected by J. Běluša in the 1960s during active mining and were provided by the Moravian Museum, Brno from its mineralogical collection. Most samples from the Věžná I pegmatite were obtained in the Moravian Museum and several samples were collected by the authors as were all samples of beryl from Kovářová.

Electron-probe microanalyses (EPMA)

Chemical analyses of studied phases were performed on carbon-coated epoxy mounts using a Cameca SX-100 electron-probe microanalyzer in wavelength-dispersive mode. The following analytical conditions were used for zeolites (and other phases, respectively):

accelerating voltage of 15 kV, beam current of 4 nA (10 nA), and beam diameter of 10 μm (5 μm). The following natural and synthetic standards were used for quantification: albite (Na), sanidine (K, Al, Si), pyrope, (Mg), almandine (Fe), spessartine (Mn); wollastonite (Ca), titanite (Ti), topaz (F), vanadinite (Pb, Cl), Ni_2SiO_4 (Ni), gahnite (Zn), baryte (Ba), $SrSO_4$ (Sr). Peak counting times (CT) were 10 s for main elements and 20–40 s for minor elements; CT for each background was one-half of the peak CT. The raw intensities were converted to the concentrations using X-PHI (Merlet, 1994) matrix-correction software involving the theoretical amount of unanalysed oxides in the correction routine.

Micro-Raman spectroscopy

Minerals in grains several mm to several μm across found in polished sections were very difficult, if not impossible, to characterize by X-ray diffraction and thus were studied by Micro-Raman spectroscopy. This method was used as a supplementary technique to the WDS analysis to confirm the phase identification of selected minerals. Single Raman spectra analyses were obtained at room temperature by means of a Horiba Jobin Yvon LabRam-HR Evolution at the Department of Geological Sciences, Masaryk University, Czech Republic. Raman spectrometer was equipped with a Si-based, Peltier-cooled charge-coupled device detector, coupled to an Olympus BX41 microscope and diffraction grating with 1800 grooves per millimetre. Spectra were mainly excited with the 473 nm emission of a diode laser. Attempts to obtain new Raman spectra were also made with 532, 633 and 785 nm laser excitation to verify the measurements and to eliminate possible analytical artefacts caused by laser-induced photoluminescence. The instrument was calibrated using the Rayleigh line, resulting in a 0.5 cm^{-1} wavenumber accuracy. An Olympus 100× objective (numerical aperture 0.90) was used, whereby spectra were obtained in a range of 100-3800 cm^{-1} in confocal mode; the lateral resolution was better than 1 μm. The spectral resolution was better than 1.2 cm^{-1}. Data were processed with Seasolve PeakFit 4.12 and LabSpec 6 software. Band fitting was done after appropriate background correction, assuming Lorentzian-Gaussian band shapes.

6. Results

6.1. Paragenetic types and chemical composition of primary and secondary beryl

This chapter provides a brief information about paragenetic position (host textural-paragenetic unit) and mineral assemblages of primary beryl in the examined pegmatites based on our research and in part also on the published data (see Table 2; Drahonín IV – Sojka,

1969; Novák *et al*., 2023a; Věžná I – Černý, 1963, 1965, 1968; Novák *et al*., 1991; Toman and Novák, 2018, 2020, Dolní Rožínka - Novotný and Cempírek, 2021, Kovářová - Přikryl *et al*., 2012, 2014). Also, subsolidus recrystallization of primary beryl to secondary beryl (Cs-enriched beryl to pezzottaite) as late veinlets or irregular masses is briefly mentioned, as well as chemical compositions of secondary recrystallized beryl from Věžná I and Kovářová.

Our description of the paragenetic position of beryl from the Drahonín IV pegmatite is based on the data presented by Sojka (1969) and chiefly on the detailed study of numerous samples from the Moravian Museum, Brno. Large hexagonal prisms of beryl I, up to ~40 cm long and ~15 cm thick, occurred in strongly albitized blocky K-feldspar and they were often almost completely dissolved. Rare crystals of homogeneous beryl II, up to 3 cm in size, associated with spessartine in albite unit were moderately altered (Fig. 5a). Both beryl I and beryl II were replaced by a rich assemblage of secondary minerals but no recrystallization to secondary beryl was observed perhaps because relics of primary beryl I and beryl II are very rare in the studied samples. The Věžná I pegmatite contains three distinct paragenetic types of primary beryl (Table 2, Toman and Novák, 2020). The most abundant greyish beryl II as large subhedral to euhedral crystals, up to 20 cm long and 5 cm thick, in intermediate blocky unit and albite (Novák *et al*., 1991; Toman and Novák, 2020) is locally recrystallized (Fig. 5b) to beryl IIA (Cs-enriched beryl) and frequently replaced by fine-grained aggregates of secondary phases (Černý, 1968; Novák *et al*., 1991; this work).

The chemical composition of primary and secondary recrystallized beryl from the individual localities is presented in Table 3 and Fig. 6. At the most evolved Dolní Rožínka and Věžná I pegmatites the individual types of primary beryl evolved from Na,Fe,Mg-enriched compositions to Cs-enriched ones. Relics of beryl II from the Drahonín IV pegmatite are close to the ideal composition with low Fe and Na contents. Compositional evolution from primary beryl to recrystallized secondary beryl exhibits an obvious trend from Cs-enriched beryl (Věžná I) to Cs-enriched beryl and pezzottaite (Dolní Rožínka; Fig. 5c). In the pegmatite Kovářová, several textural and compositional types of secondary beryl were described by Přikryl *et al*., (2012, 2014). Primary beryl I and beryl II have similar composition and are enriched in Cs, Na, Fe and Mg; rims of secondary beryl IA (Fig. 5d) are slightly Mg-enriched.

6.2. Assemblages of secondary minerals after beryl

The individual localities differ significantly in the degree of hydrothermal alteration and in the assemblages of secondary minerals after beryl (Table 4). We focused mainly on the

proximal assemblages of secondary Be-minerals in the sense of Novák *et al*., (2015b, 2023a) because distal secondary Be-minerals on tectonic fractures and fissures are known only from the Věžná I pegmatite where they typically occur on fractures situated close to strongly altered Be-enriched cordierite. These secondary Be-minerals (milarite, bohseite) are very likely related to its hydrothermal alteration (Černý and Povondra, 1966, 1967; Gadas *et al*., 2020; Toman and Novák, 2020; Novák *et al*., 2023a).

Four distinct assemblages of secondary minerals after beryl were recognized at the Drahonín IV pegmatite (Table 4). (D-i) Very abundant and most advanced secondary assemblage is developed in the secondary pockets after large, dissolved crystals of beryl I and exceptionally in their very close vicinity (<1-2 cm); relics of beryl I are extremely rare. Bavenite-bohseite is a dominant secondary Be-mineral, along with less abundant euhedral grains of bertrandite arranged in belts or irregularly distributed as euhedral grains enclosed in and locally replaced by host bavenite-bohseite (Fig. 7a,b). Bavenite-bohseite also forms colourless tabular crystals and their aggregates with abundant pyrite. This assemblage also contains several rare accessory minerals. Euhedral grains of cassiterite (Fig. 7c), xenotime-(Y) and microlite-group mineral are very likely inclusions in the primary beryl I. Abundant chlorite and very rare pyrite, sphalerite, galena, Sn-rich titanite, titanite, and stokesite are secondary phases associated with the secondary Be-minerals, which volumetrically predominate over the secondary Be-free phases. Less advanced replacement assemblages after beryl II are characterized by complex mineralogy and textural relations (Table 4, Fig. 7d,e,f). (D-ii) Numerous veinlets of bavenite-bohseite ± analcime, contain also minor euhedral bertrandite, and gismondine-Ca, and rare chlorite, laumontite, scolecite-Ca, and pyrite (Fig. 7d,e). (D-iii) The assemblage Btd + Kfs with rare hydroxylgugiaite was found only in a few places. (D-iv) Very rare veinlet in beryl II, zoned milarite (locally Y-enriched) + bavenite-bohseite + quartz + K-feldspar + muscovite + chlorite (Fig. 7f) is spatially closely associated with an elongated grain of primary cassiterite; bertrandite is absent in the (iv) assemblage (Table 4). Absence of spatial relations of the separately distributed individual secondary mineral assemblages in the Drahonín IV pegmatite described above does not allow to distinguish their sequential relations.

At the Věžná I pegmatite, the individual assemblages of proximal secondary Be-minerals after beryl II are very complex (Fig. 8; Table 4) but in contrast to the Drahonín IV pegmatite, they locally show evident sequential relations. The assemblage (V-i) Kfs + Btd in thin irregular veinlets is the most abundant; locally harmotome (Fig. 8a) and heulandite-Ca are associated. Rare to very rare baryte, arsenopyrite, löllingite, Fe_3SbAs_6 phase + secondary

scorodite are only locally present in these veinlets (Fig. 8b). On the contact of beryl II and zoned and fractured tourmaline crystal thin veinlets of the (V-i) assemblage are developed. They differ by the absence of bertrandite in K-feldspar veinlets cutting the schorl grain; hence, the occurrence of bertrandite is restricted solely to the replaced beryl crystal (Fig. 8d). (V-ii) Minor veins of epidydimite crosscut the (V-i) veinlets Kfs + Btd (Fig. 8b,c,e). Epidydimite is associated with less abundant hydroxylgugiaite, baryte, and heulandite-Ca (Fig. 8f; Table 4). Both early veinlets (V-i) and veins (V-ii) are cut by (V-iii) long and thin veins of late hydroxylgugiaite + K-feldspar, where hydroxylgugiaite is commonly developed in outer parts of these veins (Fig. 8f). The complex textures characteristic of the rarer minerals do not obscure the relationships defining the sequence (V-i) → (V-ii) → (V-iii).

In the Dolní Rožínka pegmatite alterations of beryl are weak disregarding very common recrystallized secondary beryl (Cs-rich beryl to pezzottaite; Fig. 5c); very rare bertrandite is the only proximal secondary Be-mineral in small secondary pocket after dissolved beryl from cleavelandite (Novotný and Cempírek, 2021). No secondary Be-minerals were observed in beryl I the Kovářová pegmatite (Fig. 5d), disregarding heterogeneous recrystallized beryl IIA which hosts numerous inclusions of Cs-rich annite and muscovite (Přikryl *et al.*, 2014).

6.3. Chemical composition of secondary Be-minerals

Some secondary Be-minerals are close to their ideal formulae (bertrandite). Epididymite as well as hydroxylgugiaite have minor to trace concentrations of FeO, MgO, SrO, and Rb_2O (Table 5). Only bavenite-bohseite and milarite from Drahonín IV are rather heterogeneous showing moderate variation in Al and Y, respectively (Table 5). The associated Be-free secondary minerals (Table 3) usually yielded standard chemical compositions close to the ideal formulae with no notable variations; only secondary K-feldspar (≤0.39 wt.% BaO) associated with bertrandite and locally with harmotome from the Věžná I pegmatite is Ba-enriched (Fig. 8a).

6.4. Raman spectroscopy of secondary minerals

A spectroscopic study focused on identifications of microscopic grains of secondary Be-minerals (compared with already known spectra in the RRUFF database – Lafuente *et al.*, 2015) revealed the following minerals – quartz, tourmaline (elbaite type – for comparison see Huy *et al.*, 2011), albite, K-feldspar, beryl, bertrandite, bavenite, bohseite and hydroxylgugiaite (Fig. 9). Detailed study of bavenite-bohseite solid solution found that spectra for the Drahonín IV and Věžná I pegmatites differ. Based on vibrations in the OH

region, the bavenite-bohseite from the Drahonín IV locality corresponds to 1:1 bavenite-bohseite composition (similar spectra to a pegmatite at Ruprechtice - see also Novák *et al.*, 2023a) whereas by studying a different sample from Věžná I, the spectrum was typical for distal bohseite as described at the Věžná I. in Novák *et al.*, (2023a). Raman spectra of hydroxylgugiaite are similar at both localities.

7. Discussion

The alteration products after primary beryl and other primary minerals from several granitic pegmatites located along the boundary of the Strážek Unit and Svratka Crystalline Unit (Fig. 1) are very distinct including their textural and paragenetic relations (Table 1,2,4). Consequently, they may disclose sources of fluids which facilitated the origin of these proximal assemblages of secondary Be-minerals including recrystallization generating secondary beryl. The role of compositionally contrasting host rocks and fine brittle tectonics also are discussed.

7.1. Assemblages of secondary minerals after beryl

Identification of the individual secondary minerals on BSE images supported by EDS spectra and subsequent WDS analyses is the major method; however, we found that this approach is not always sufficient. Micro-Raman spectroscopy provides significant advantages over other used analytical techniques in this study discussed below, and its compatibility with optical microscopy is a noteworthy benefit (Araujo *et al*., 2020; Groppo *et al*., 2006). Based on this compatibility, we were able to distinguish phases of different secondary Be-minerals from other minerals, especially in the case of discerning K-feldspar from hydroxylgugiaite (Fig. 10). This can be a significant issue for distinguishing phases in pegmatites by using the BSE imaging (Schulz *et al*., 2020), as gugiaite or hydroxylgugiaite can be could be more widespread but overlooked (Grice *et al*., 2017).

The examined pegmatites differ significantly in the assemblages of secondary minerals after primary beryl (Table 4). Recrystallizations of primary beryl to secondary beryl is the earliest process and it was most extensive at Kovářová, where secondary beryl IIA volumetrically predominates over primary beryl II (Přikryl *et al.* 2014), less extensive at Dolní Rožínka, only moderate at Věžná I and Kovářová beryl I, and absent in Drahonín IV (Fig. 5), although scarcity of beryl relics at Drahonín IV partly obsures this trend. The secondary beryl IIA from the Kovářová pegmatite with common inclusions of micas (Přikryl *et al*., 2014) differs significantly in the texture and mineral assemblage and was not discussed in detail.

The abundances of proximal secondary Be-minerals in the individual localities differ considerably. The highest grade of alterations was evidently achieved in the Drahonín IV pegmatite. Bavenite-bohseite + minor bertrandite are dominant in the (D-i) assemblage after beryl I (Fig. 7a,b). The secondary assemblages after less altered beryl II are more variable and include dominant (D-ii) assemblage bavenite-bohseite + minor analcime, rare bertrandite, zeolites, and rare sulphides (Fig. 7c,d), rare (D-iii) bertrandite + K-feldspar ± hydroxylgugiaite (Fig. 7e) and very rare (D-iv) assemblage milarite ± bavenite-bohseite (Fig. 7f).

The grade of primary beryl II alterations in the Věžná I pegmatite is strong to weak; complete to almost complete dissolution of primary beryl crystals similar to Drahonín IV was not observed (see also Novák *et al*., 1991; Toman and Novák, 2020). Also, the assemblages of proximal secondary minerals are different showing at least 3 successive stages locally documented by evident crosscutting textures (Fig. 8b,c,e,f). The most abundant assemblage is (V-i) bertrandite + K-feldspar ± harmotome (Fig. 8a) along with less abundant assemblages (V-ii) epidydimite + hydroxylgugiaite + rare baryte, and (V-iii) hydroxylgugiaite + K-feldspar (Fig. 8f). These individual assemblages from Věžná I differ from the Drahonín IV pegmatite in locally evident succession of crystallization (Fig. 8b,c,e,f) and presence of epididymite, abundance of hydroxylgugiaite and locally Ba-enriched minerals (harmotome, K-feldspar) (Fig. 8a,c).

The mineral assemblages in Table 4 evidently show that Ca + Be (bavenite-bohseite > bertrandite > Ca-zeolites) are dominant cations in the secondary minerals from Drahonín IV along with minor to rare K (K-feldspar) and Na (analcime). In contrast the Věžná I pegmatite shows dominant Be + K (bertrandite, K-feldspar) and moderate to minor Ca (hydroxylgugiaite, heulandite-Ca), Ba (harmotome, baryte) and Na (epidydimite). At the Dolní Rožínka pegmatite, only Be is present in rare secondary bertrandite. Traces of Zn, Pb, Fe, Ti and Sn in rare secondary minerals are typical in Drahonín IV as well as the participation of S in sulphides. In the Věžná I pegmatite, traces of As + S in rare arsenopyrite, löllingite, Fe_3SbAs_6 phase and secondary scorodite were found. Different textural relations at the Drahonín IV and Věžná I pegmatites showing spatial *versus* sequential assemblages, distinct mineral assemblages and geochemical signature of secondary minerals (Table 4) manifest different types and availability of fluids which facilitated the origin of secondary minerals after beryl as well as they implied distinct sources of fluids (see below).

7.2. RAMAN spectra of hydroxylgugiaite

Most of the identified minerals have characteristic Raman spectra without the presence of any abnormalities. A unique occurrence of the mineral hydroxylgugiaite in the granitic pegmatites was confirmed by micro-Raman spectroscopy. Given the vibrational features of structure and its classification in the melilite group (Grice *et al*., 2017), the possible tentative assignments were made based on similarities with other minerals from this group. Part of the spectrum in the low-frequency region from 300 cm^{-1} to 600 cm^{-1} represents bands of various forms of deformation vibrations and translational vibrations of big structural units and cations associated with (Si,Be,Al)O_3 units (Fig. 9). At 676 cm^{-1}, high-intensity band corresponding to the symmetric stretching mode of the bridging oxygen in the Si_2O_7 dimer occurs. The Raman band at 960 cm^{-1} probably involves the contribution of the [(Si,Be)O_4] stretching. Other Raman bands in the range between 800–1100 cm^{-1} should be related to pyrosilicate unit for nonbridging and bridging stretching modes (for comparison see Sharma *et al*., 1988). Since hydroxylgugiaite is incorporating a hydrogen atom, we were able to detect OH^- vibrational modes at the 3572, 3615 and 3643 cm^{-1}. Based on the correlation of O–H stretching frequencies and O–H· · ·O bond lengths, the frequency range for hydroxylgugiaite most likely corresponds to the distance value for *d*(H· · ·O) around 2.3 Å (Libowitzky, 1999) which coincides with weak hydrogen bonds to two *O*3 sites observed by Grice *et al.,* (2017).

7.3. Textural characteristics of beryl replacement

The individual localities differ significantly in the textural development of replacement processes. Microscopic, irregular, long and thin fractures (< 0.5 mm) cutting grains of primary beryl II typically predominate in the Věžná I pegmatite whereas in the Drahonín IV pegmatite almost total breakdown of a large crystal of beryl I (several dm^3) is characteristic. Also, no sequential processes disregarding minor alteration of bertrandite crystals by bavenite-bohseite (Fig. 7b) were observed in beryl I from the Drahonín IV pegmatite and suggest extensive action of fluids as well as their variability. Evident crosscutting textures in large beryl II crystals from the Věžná I pegmatite (Fig. 8b,c,e,f) indicate several sequential and rather independent hydrothermal substages although such evident sequential behaviour was not observed in all examined samples.

Because zeolites and extensive alterations were not found in other pegmatites of the Strážek Unit (Novák *et al*., 2015a), tectonic processes along the border of Strážek Unit and Svratka Crystalline Unit played a significant role in the alteration chiefly at the examined pegmatites Drahonín IV, Věžná I, Věžná II (Černý, 1963, 1965, 1968; Novák *et al*., 2023a) and in the barren pegmatite Domanínek near Bystřice nad Pernštejnem (Novák *et al*., 2023b).

All these pegmatites are situated at the Olší shear zone (Drahonín IV), close to it (Věžná I, Věžná II), or close to other subparallel less important shear zones (Domanínek). Tectonic fracturing of host pegmatite was necessary for an effective fluid flow and subsequent replacement processes.

7.4. PTX conditions

Very complex and typically evident disequilibrium assemblages of secondary minerals at the individual pegmatites (Fig. 5, 7, 8, 10) enable only an approximation of *PTX* conditions of the alteration processes based on the experimentally obtained stabilities for some secondary minerals (e.g., Barton, 1986; Barton and Young, 2002; Chipera and Apps, 2001; Frey and Robinson, 2009; Weisenberger and Bucher, 2010, 2011). Recrystallization of primary beryl to secondary beryl (typically Cs-enriched beryl to pezzottaite) with none to very low Mg contents, as well as the observed textures (Fig. 5b,c) indicate that this process proceeded before opening the pegmatite, or at least the relevant part of pegmatite body containing primary beryl, to the fluids from Mg-rich host rocks (serpentinite, dolomite marble; Table 1). The conditions at T ~300-400 °C and P <~ 200-300 MPa, corresponding to lithostatic pressure of the pegmatite melt emplacement assumed for the rare-element granitic pegmatites of the Moldanubian Zone (Ackermann *et al*., 2007; Novák *et al*., 2013, 2015a), were estimated for this beryl recrystallization process (see also London, 2008; Novák *et al*., 2023a; Chládek *et al*., 2024).

The assemblage (i) bertrandite + K-feldspar is rare in Drahonín IV but abundant in the Věžná I pegmatite. Bertrandite is stable at T < 240 °C, P = 100 MPa and low activity of Al according to Barton (1986) and Barton and Young (2002) (Fig. 11). However, the recent study of bavenite-bohseite and its mineral assemblages including the abundant assemblage K-feldspar + bertrandite revealed that the temperature of bertrandite crystallization may be shifted up to T ~ 300 °C and its stability to at least moderately alkaline conditions (Novák *et al*., 2023a). Rims around K-feldspar enriched in Ba (Fig. 8a) may be related to precipitation of low-T harmotome. Alkaline conditions are supported by the occurrence of abundant zeolites at the Drahonín IV and at Věžná I pegmatites (Table 4; Toman and Novák, 2018; Novák *et al*., 2023b) as well as the associated hydroxylgugiaite (Fig. 8f, 10). The bertrandite assemblages with secondary Be-minerals (e.g., epididymite, hydroxylgugiaite, behoite, leucophanite) typical mainly for syenite pegmatites (Grice *et al*., 2017 and references therein) support an alkaline environment as well. Moreover, evident crosscutting textures in the Věžná I pegmatite show that the early assemblage (V-i) bertrandite + K-feldspar is followed by

rather alkaline assemblages (V-ii) with epididymite and (V-iii) with hydroxylgugiaite. Consequently, the acidity/alkalinity of fluids may vary significantly in time and space mainly at the Věžná I pegmatite. The T < ~200-300 °C is feasible for the early assemblage K-feldspar + bertrandite; however, occurrence of zeolites associated with bertrandite + K-feldspar (harmotome) and with epididymite rather support lower T <~150-200 °C and hydrostatic pressure P <~0.5 MPa. Moreover, widespread occurrences of harmotome in Věžná I (Teertstra *et al*., 1995; Toman and Novák, 2020; Novák *et al*., 2023a) synthetized at T = 95 °C (Perrotta, 1976) indicates low T ~100 °C as well.

7.5. Potential sources of acting fluids for the individual secondary mineral assemblages

Evident differences in the degree of hydrothermal alterations, textural relations, mineral assemblages, as well as in the chemical composition of secondary minerals including Be-rich and Be-free phases, imply different sources and availability of fluids which facilitated the breakdown of primary ± recrystallized secondary beryl in the individual pegmatites examined. Zeolites were not observed in other granitic pegmatites of the Strážek Unit (Novák *et al*., 2015a) and they were described only from the pegmatites situated along its E border (Černý 1965, Pauliš and Cempírek, 1998; Toman and Novák, 2018; Novák *et al*., 2023b). Consequently, tectonic fracturing and availability of fluids along the border of Strážek Unit and Svratka Crystalline Unit played a significant role in the alteration processes chiefly in the Drahonín IV and Věžná I pegmatites situated close to or directly in the Olší shear zone (Fig. 2).

Secondary recrystallized beryl

Irregular veinlets and aggregates of secondary beryl in primary beryl were described from large LCT granitic pegmatites e.g., Bikita, Zimbabwe (Černý *et al*., 2003) and Koktokay No.3, China (Wang *et al*., 2009) as well as from small NYF pegmatites (e.g., Kožichovice II, Třebíč Pluton; Novák and Filip, 2010; Zachař *et al*., 2020) and LCT pegmatite (e.g., Maršíkov D6e; Chládek *et al*., 2024). Secondary beryl is Na,Cs,(Li)-enriched and Fe,Mg-poor at two large and highly evolved pegmatites mentioned above whereas it is depleted in Na, Fe and Mg relative to the primary beryl in Kožichovice II but Na,Fe,Mg-enriched in the D6e pegmatite, Maršíkov (Chládek *et al*., 2024). In the examined localities secondary beryl (Cs-enriched beryl to pezzottaite in Dolní Rožínka) shows elevated concentrations of Cs but very low Mg (Novotný and Cempírek, 2021, Fig. 5c). In the Věžná I pegmatite low contents of Mg in secondary beryl IIA may have been sourced from primary Mg-enriched beryl II (Fig. 6a; Table 3). Consequently, the origin of secondary beryl after primary beryl in most granitic

pegmatites including the examined pegmatites was very likely facilitated by residual pegmatite fluids in the system closed to the host rock. It is supported by the textures, elevated concentrations of Cs and the absence or very low contents of Mg in the recrystallized secondary beryl, although the examined pegmatites are typically enclosed in Mg-rich rocks (Table 1). In contrast, elevated Mg in secondary beryl and overall assemblage of secondary minerals including chlorite in the pegmatite D6e, Maršíkov (Chládek *et al*., 2024) suggest participation of external fluids in the secondary beryl origin. However, the Maršíkov district displays strong tectonic/metamorphic overprint (Černý *et al*., 1992; Rybnikova *et al*., 2023) significantly distinct from the examined region. Only beryl I from Kovářová contains narrow rims of recrystallized Mg-enriched beryl IA and is texturally similar to the Maršíkov D6e pegmatite (Chládek *et al*., 2024).

Secondary Be-minerals in Drahonín IV

Rather alkaline character of the beryl alterations from Drahonín IV is indicated by common zeolites and differs significantly from the alterations of beryl described in other examined granitic pegmatites from the Strážek Unit and other regions of the Moldanubian Zone (e.g., Novák *et al*., 2013, 2015a, 2023b; Přikryl *et al*., 2014; Gadas *et al*., 2016, 2020). Textures and mineral assemblages (muscovite + Mn-rich chlorite + albite) in the veins after altered garnet at Drahonín IV and their geochemical signature also are very distinct from altered garnets in the Li-bearing granitic pegmatites of the Moldanubian Zone where they are locally replaced along their rims by blue Fe-rich fluor-elbaite (Buřival and Novák, 2018; unpubl. data of the authors) and/or by zinnwaldite-masutomilite mica (Němec, 1990); however, dominant participation of residual pegmatite fluids is evident in the Li-poor pegmatite Drahonín IV and in Li-bearing pegmatites as well. Calcium is a dominant cation (bavenite-bohseite, gismondine-Ca, laumontite, scolecite-Ca, apatite, hydroxylgugiaite) along with minor Na (analcime, albite) and rare K (muscovite, K-feldspar) in the Drahonín IV pegmatite (Table 4). Almost total breakdown of large beryl crystal, abundant pyrite + chlorite, and rare sphalerite and galena typically associated with dominant bavenite-bohseite as well as calcite and pyrite ongrowing crystals of quartz from large miarolitic pocket (Sojka, 1969) suggest a massive flow of fluids enriched in Ca, Na, Fe, Pb, Zn, CO_2 and S. Strong alteration to a total breakdown of primary beryl I, absence of Ba-rich minerals, occurrence of sulphides as well as high-T of the alteration process estimated from the mineral assemblages (Table 4) indicate that it is likely related to the pre-uranium quartz-sulphide and carbonate-sulphide mineralization defined in this region by Kříbek *et al*. (2009) with similar geochemical signature. It is also supported by a close spatial relation of the Drahonín IV pegmatite to the

NNW–SSE striking shear zone Olší associated with hydrothermal mineralizations at the Rožná-Olší ore field (e.g., Kříbek *et al*., 2009; Wertich *et al*., 2022; Novák *et al*., 2023b). Also, early zeolite and apophyllite assemblages from the Rožná-Olší ore field examined by Novák *et al*. (2023a) exhibit similar geochemical signature of fluids and are very likely related to the pre-uranium quartz-sulphide and carbonate-sulphide mineralizations (see Kříbek *et al*., 2009).

Secondary Be-minerals in Věžná I

Multistage evolution and geochemical characteristics observed at the Věžná I pegmatite suggest that these alteration processes were different from the Drahonín IV pegmatite. Mostly microscopic crosscutting veins and veinlets, although typically proximal to the replaced beryl II, manifest an important role of fine fracturing on a microscopic scale. Rather minor participation of Ca (hydroxylgugiaite) but high K (K-feldspar), moderate Na (epidydimite) and locally high Ba (harmotome, baryte, Ba-enriched K-feldspar) as well as traces of As, Fe, Sb and S indicate different sources of fluids comparing the Drahonín IV pegmatite. Mineral assemblages of zeolites on tectonic fractures and fissures from this pegmatite (Novák *et al*., 2023b) have similar geochemical signature. Participation of fluids generated during a retrograde stage of the Variscan metamorphism is feasible. Alternatively, a contribution of low-temperature highly alkaline fluids responsible for a large-scale HFSE and REE remobilization from (ultra)potassic plutons related to the formation of Moldanubian U-deposits is possible as well (Kubeš *et al*., 2021, 2024). However, traces of As, S and Sb indicate also other source. Because löllingite and arsenopyrite are quite abundant accessory minerals in most granitic pegmatites from the Strážek Unit (Novák *et al*., 2015a; Novotný and Cempírek, 2021), residual pegmatite fluids are a potential source of As, S and Sb along with K > Ca, Na > Ba. Because similar assemblages of secondary Be-minerals in the Věžná II pegmatite (Černý, 1965; Pauliš and Cempírek, 1998; Novák *et al*., 2023b) and zeolites (phillipsite-Ca to harmotome, thomsonite-Ca, rare natrolite and chabazite-K), were found in other pegmatites cutting serpentinite in the Moldanubicum (e.g., Bernartice; Sejkora *et al*., 2023) Ba may have been sourced from host rock.

Secondary Be-minerals in Dolní Rožínka and Kovářová

Very rare proximal bertrandite (As-enriched, Novotný and Cempírek, 2021) after beryl and abundant fresh beryl crystals in the Dolní Rožínka pegmatite indicate rather low participation of fluids during subsolidus processes comparing the Drahonín IV and Věžná I pegmatites. Elevated concentrations of As in bertrandite is similar to the Věžná I pegmatite where late löllingite, arsenopyrite and scorodite are associated with secondary Be-minerals in

the assemblage (V-i). Recrystallization of beryl I to slightly Mg-enriched beryl IA as well as recrystallized beryl IIA in the Kovářová pegmatite with abundant inclusions of Cs-rich annite and muscovite (Přikryl *et al*., 2014) are very different and suggest evidently different nature of the subsolidus processes in this locality situated in the Svratka Crystalline Unit (Fig. 2) comparing the examined pegmatites from Strážek Unit. Both pegmatites are situated out of the shear zones Rožná and Olší and quite far from the tectonic contact of these units (Fig. 2).

8. Conclusions and summary

Considerable fluid flow through the ductile to brittle shear zones Rožná and Olší and associated brittle tectonics along the border of the Strážek Unit and Svratka Crystalline Unit is manifested by several hydrothermal mineralizations in the U-deposits from the Rožná-Olší ore field (Kříbek *et al*., 2009; Wertich *et al*., 2022; Novák *et al.,* 2023a). Strong alterations of primary beryl I and beryl II in the Drahonín IV pegmatite (bavenite-bohseite > bertrandite) located in the Olší shear zone characterized by the presence of sulphides (pyrite, galena, sphalerite) and zeolites (analcime, gismondine-Ca, laumontite, scolecite-Ca) is very likely related to the pre-uranium quartz-sulphide and carbonate-sulphide mineralizations defined by Kříbek *et al*. (2009). Almost total replacement of large beryl I crystal required a massive fluid flow manifested by several stages of hydrothermal mineralizations at this ore field (Kříbek *et al*., 2009; Novák *et al*., 2023b).

Alterations of beryl II in the Věžná I pegmatite showing several distinct and crosscutting textures of the individual substages (bertrandite + K-feldspar; epidydimite + K-feldspar; hydroxylgugiatite + K-feldspar) including rare Fe-sulphides and arsenides are rather controlled by postmagmatic residual fluids (recrystallized secondary beryl, early assemblage bertrandite + K-feldspar) followed by fluids related to a retrograde stage of metamorphism of compositionally contrasting host serpentinite. The pegmatites Dolní Rožínka and Kovářová located out of the shear zones (Fig. 2) exhibit only a low degree of alterations in Dolní Rožínka facilitated by residual fluids (As-enriched bertrandite) and different compositional, textural and paragenetic development in the Kovářová pegmatite located in the Svratka Crystalline Unit.

Micro-Raman spectroscopy is a suitable technique to identify and distinguish hydroxylgugiaite, as well as other Be-minerals such as bavenite-bohseite solid solution (Novák *et al*., 2023b), bertrandite, and beryl, mostly present in the studied samples. The uncommon hydroxylgugiaite, hardly distinguishable from K-feldspar in the BSE images, could be distinguished optically (textures and habitus of crystals) or utilizing Raman spectroscopy and was likely overlooked in some previous studies. Hydroxylgugiaite was

described for the first time by a unique set of Raman bands with OH present in the region around 3600 cm^{-1}.

Highly variable assemblages of secondary minerals after beryl frequently unstable in subsolidus conditions are perfect mineral indicators of hydrothermal overprint during subsolidus processes including residual fluids and external fluids of various origin. However, the scarcity of beryl in nature makes its wide usage limited in the study of subsolidus hydrothermal processes in general.

Acknowledgments

The authors thank E. Grew and two anonymous reviewers for constructive criticism that significantly improved the manuscript and V. Wertich for technical assistance. This research was supported by OP RDE [grant number CZ.02.1.01/0.0/0.0/16_026/0008459 (Geobarr) from the ERDF] for MN. This work also appears through the institutional support of long-term conceptual development of research institutions provided by the Ministry of Culture (ref. MK000094862) for JT.

References

Ackerman L., Zachariáš J. and Pudilová M. (2007) P–T and fluid evolution of barren and lithium pegmatites from Vlastějovice, Bohemian Massif, Czech Republic. *International Journal of Earth Sciences,* 96, 623–638.

Ackerman L., Haluzová E., Creaser R. A., Pašava J., Veselovský F., Breiter K., Erban V. and Drábek M. (2017) Temporal evolution of mineralization events in the Bohemian Massif inferred from the Re–Os geochronology of molybdenite. *Mineralium Deposita,* 52, 651–662.

Araujo P. F., Hulsbosch N. and Muchez P. (2020) High spatial resolution Raman mapping of complex mineral assemblages: Application on phosphate mineral sequences in pegmatites. *Journal of Raman Spectroscopy*, 52(3), 690–708. doi:10.1002/jrs.6040

Barton M. (1986) Phase equilibria and thermodynamic properties of minerals in the BeO-Al_2O_3-SiO_2-H_2O (BASH) system, with petrologic applications. *American Mineralogist,* 71, 277–300.

Barton M. and Young S. (2002) Non-pegmatitic deposits of beryllium: mineralogy, geology, phase equilibria and origin. Pp. 591–691 in: *Beryllium – mineralogy, petrology and geochemistry* (E.S. Grew, editor). Reviews in Mineralogy and Geochemistry, 50. Mineralogical Society of America, Washington DC.

Buriánek D. and Novák M. (2007) Compositional evolution and substitutions in disseminated and nodular tourmaline from leucocratic granites: Examples from the Bohemian Massif, Czech Republic. *Lithos*, 95, 148–164.

Buriánek D., Dolníček Z. and Novák M. (2016) Textural and compositional evidence for a polyphase saturation of tourmaline in granitic rocks from the Třebíč pluton (Bohemian massif). *Journal of Geosciences*, 61(4), 309–334.

Burnham C. W. and Nekvasil H. (1986) Equilibrium properties of granite pegmatite magmas. *American Mineralogist*, 71(3-4), 239–263.

Burt D. (1978) Multisystems analysis of beryllium mineral stabilities: the system BeO-Al_2O_3-SiO_2-H_2O. *American Mineralogist,* 63, 664–676.

Buřival Z. and Novák M. (2018) Secondary blue tourmaline after garnet from elbaite-subtype pegmatites; implications for source and behaviour of Ca and Mg in fluids. *Journal of Geosciences*, 63(2), 111–122.

Cempírek J., Novák M., Dolníček Z., Kotková J. and Škoda R. (2010) Crystal chemistry and origin of grandidierite, ominelite, boralsilite, and werdingite from the Bory Granulite Massif, Czech Republic. *American Mineralogist*, 95, 1533–1547.

Černý P. (1963) Epididymite and milarite – alteration products of beryl from Věžná, Czechoslovakia. *Mineralogical Magazine*, 33, 450–457.

Černý P. (1965) *Mineralogy of two pegmatites from the Věžná serpentinite*. CSc thesis, Geological Institute of the ČSAV Prague, Prague, Czechoslovakia. Pp. 1–177. (in Czech)

Černý P. (1968) Berylliumwandlungen in Pegmatiten - Verlauf und Produkte. *Neues Jahrbuch für Mineralogie, Abhandlungen,* 108, 166–180.

Černý P. (2002) Mineralogy of beryllium in granitic pegmatites. Pp. 405–444 in: *Beryllium – mineralogy, petrology and geochemistry* (E.S. Grew, editor). *Reviews in Mineralogy and Geochemistry*, 50. Mineralogical Society of America, Washington DC.

Černý P. and Ercit T.S. (2005) The classification of granitic pegmatites revisited. *The Canadian Mineralogist*, 43, 2005–2026.

Černý P. and Miškovský L. (1966) Ferroan phlogopite and magnesium vermiculite from Věžná, Westrn Moravia. *Acta Universitatis Carolinae, Geologica*, 2, 17–32.

Černý P. and Povondra P. (1966) Beryllian cordierite from Věžná: (Na,K) + Be=Al. *Neues Jahrbuch für Mineralogie, Monatshefte*, 36–44.

Černý P. and Povondra P. (1967) Cordierite in West-Moravian desilicated pegmatites. *Acta Universitatis Carolinae, Geologica*, 3, 203–221.

Černý P., Novák M. and Chapman R. (1992) Effects of sillimanite-grade metamorphism and shearing on Nb-Ta oxide minerals in granitic pegmatites: Maršíkov, Northern Moravia, Czechoslovakia. *The Canadian Mineralogist*, 30, 699–718.

Černý P., Novák M. and Chapman R. (2000) Subsolidus behavior of niobian rutile from Věžná, Czech Republic: a model for exsolution in phases with Fe^{2+} >> Fe^{3+}. *Journal of the Czech Geological Society*, 45, 21–35.

Černý P., Anderson A. J., Tomascak P.B. and Chapman R. (2003) Geochemical and morphological features of beryl from the Bikita granitic pegmatite, Zimbabwe. *The Canadian Mineralogist*, 41, 1003–1011

Černý, P., Smith, J.V., Mason, R.A. and Delaney, J.S. 1984. Geochemistry and petrology of feldspar crystallization in the Vezna pegmatite, Czechoslovakia. *The Canadian Mineralogist*, 22, 631–651.

Černý P., London D. and Novák M. (2012) Granitic pegmatites as reflection of their sources. *Elements*, 8, 289–294

Chipera S.J. and Apps J.A. (2001) Geochemical stability of natural zeolites. Pp. 117–161 in: *Natural zeolites: occurrences, properties, applications* (D.L. Bish and D.W. Ming, editors). *Reviews in Mineralogy and Geochemistry*, 45. Mineralogical Society of America, Washington DC.

Chládek Š., Uher P., Novák M., Bačík P. and Opletal T. (2021) Microlite-group minerals: tracers of complex post-magmatic evolution in beryl–columbite granitic pegmatites, Maršíkov District, Bohemian Massif, Czech Republic. *Mineralogical Magazine*, 85(5), 725–743.

Chládek Š., Novák M., Uher P., Gadas P., Matýsek D., Bačík P. and Škoda R. (2024) Evolution of beryllium minerals in granitic pegmatite Maršíkov D6e, Czech Republic: Complex breakdown of primary beryl by internal and external hydrothermal-metamorphic fluids. *Geochemistry*, 126092.

Čopjaková R., Prokop J., Novák M., Losos Z. and Gadas P. (2021) Hydrothermal alterations of tourmaline from pegmatitic rocks enclosed in serpentinites; multistage processes with distinct fluid sources. *Lithos,* 380, 105823.

Dosbaba M. and Novák M. (2012) Quartz replacement by "kerolite" in graphic quartz-feldspar intergrowths from the Věžná I pegmatite, Czech Republic; A complex desilicification process related to episyenitization. *The Canadian Mineralogist*, 50, 1609–1622.

Franz G. and Morteani G. (2002) Be-minerals synthesis, stability, and occurrence in metamorphic rocks. Pp. 551–598 in: *Beryllium – mineralogy, petrology and geochemistry* (E.S. Grew, editor). *Reviews in Mineralogy and Geochemistry,* 50. Mineralogical Society of America, Washington DC.

Frey M. and Robinson D. (Eds.). (2009) *Low-grade metamorphism*. John Wiley & Sons.

Gadas P., Novák M., Szuskiewicz A., Szeleg E., Galiová M.V. and Haifler J. (2016) Manganoan Na, Be, Li-rich sekaninaite from miarolitic pegmatite at Zimnik, Strzegom-Sobótka Massif, Sudetes, Poland. *The Canadian Mineralogist*, 54, 971–987.

Gadas P., Novák M., Galiová M.V., Szuszkiewicz A., Pieczka A., Haifler J. and Cempírek J. (2020) Secondary beryl in cordierite/sekaninaite pseudomorphs from granitic pegmatites – a monitor of elevated content of beryllium in the precursor. *The Canadian Mineralogist*, 58(6), 785–802.

Grew E. S., McGee J. J., Yates M. G., Peacor D. R., Rouse R. C, Huijsmans J. P. P., Shearer C. K., Wiedenbeck M., Thost D. E. and Su S.-C. (1998) Boralsilite ($Al_{16}B_6Si_2O_{37}$): A new mineral related to sillimanite from pegmatites in granulite-facies rocks. *American Mineralogist,* 83, 638–651.

Grew E.S. (2002) Beryllium in metamorphic environments (emphasis on aluminous compositions). Pp. 487–549 in: *Beryllium – mineralogy, petrology and geochemistry* (E.S. Grew, editor). *Reviews in Mineralogy and Geochemistry,* 50. Mineralogical Society of America, Washington DC.

Grice J., Kristiansen R., Friis H., Rowe R., Cooper M., Poirier G., Yang P. and Weller M. (2017) Hydroxylgugiaite: A New Beryllium Silicate Mineral From the Larvik Plutonic Complex, Southern Norway and the Ilímaussaq Alkaline Complex, South Greenland; The First Member of the Melilite Group To Incorporate A Hydrogen Atom. *The Canadian Mineralogist,* 55. 219–232. doi: 10.3749/canmin.1700002

Groppo C., Rinaudo C., Cairo S., Gastaldi D. and Compagnoni R. (2006) Micro-Raman spectroscopy for a quick and reliable identification of serpentine minerals from ultramafics. *European Journal of Mineralogy*, 18(3), 319–329. doi:10.1127/0935-1221/2006/0018-0319

Guy A., Edel J., Schulmann K., Tomek Č. and Lexa O. (2011) A geophysical Model of the Variscan orogenic root (Bohemian Massif): Implications for Modern Collisional Orogens. *Lithos*, 124, 144–157.

Hsu L.C. (1983) Some phase relationships in the system BeO-Al_2O_3-SiO_2-H_2O with comments on effects of HF. *Geological Society China Memoire*, 5, 33–46.

Huy L.H., Nguyen M.T.H., Chen B-X., Ming V.N. and Yang S.I. (2011) Raman spectroscopy study of various types of tourmalines. *Journal of Raman Spectroscopy*, 42(6), 1442–1446.

Janoušek V., Hanžl P., Svojtka M., Hora J. M., Kochergina Erban Y. V., Gadas P., Holub J.V., Gerdes A., Verner K., Hrdličková K., Daly J. S. and Buriánek D. (2020) Ultrapotassic magmatism in the heyday of the Variscan Orogeny: the story of the Třebíč Pluton, the largest durbachitic body in the Bohemian Massiff. *International Journal of Earth Sciences*, 109, 1767–1810.

Jiang S-Y., Yang J. H., Novák M., and Selway J. B. (2003) Chemical and boron isotopic compositions of tourmaline from the Lavičky leucogranite, Czech Republic. *Geochemical. Journal*, 37, 545–556.

Kotková J. (2007) High-pressure granulites of the Bohemian Massif: recent advances and open questions. *Journal of Geosciences*, 52, 45–71.

Kříbek B., Žák K., Dobeš P., Leichmann J., Pudilová M., René M., Scharm B., Scharmová M., Hájek A., Holeczy D., Hein U. F. and Lehmann B. (2009) The Rožná uranium deposit (Bohemian Massif, Czech Republic): shear zone-hosted, late Variscan and post-Variscan hydrothermal mineralization. *Mineralium Deposita*, 44(1), 99.

Kubeš M., Leichmann J., Wertich V., Mozola J., Holá M., Kanický V. and Škoda R. (2021) Metamictization and fluid-driven alteration triggering massive HFSE and REE mobilization from zircon and titanite: Direct evidence from EMPA imaging and LA-ICP-MS analyses. *Chemical Geology*, 586, 120593.

Kubeš M., Leichmann J., Buriánek D., Holá M., Navrátil P., Scaillet S. and O'Sullivan P. (2022) Highly evolved miaskitic syenites deciphering the origin and nature of enriched mantle

source of ultrapotassic magmatism in the Variscan orogenic root (Bohemian Massif, Moldanubian Zone). *Lithos,* 432–433, 106890, https://doi.org/10.1016/j.lithos.2022.106890.

Kubeš M., Leichmann J., Wertich V., Čopjaková R., Holá M., Škoda R., Kříbek B., Mercadier J., Cuney M., Deloule E., Lecomte A. and Krzemińska E. (2024) Ultrapotassic plutons as a source of uranium of vein-type U-deposits (Moldanubian Zone, Bohemian Massif): insights from SIMS uraninite U–Pb dating and trace element geochemistry. *Mineralium Deposita,* 1–38.

Lafuente B., Downs R., Yang H. and Stone N. (2015) 1. The power of databases: The RRUFF project. In T. Armbruster & R. Danisi (Ed.), *Highlights in Mineralogical Crystallography* (pp. 1–30). Berlin, München, Boston: De Gruyter (O).

Leichmann J, Gnojek I, Novák M, Sedlák J, Houzar S (2017) Durbachites from the Eastern Moldanubicum (Bohemian Massif): erosional relics of large, flat tabular intrusions of ultrapotassic melts–geophysical and petrological record. *International Journal of Earth Sciences*, 106, 59–77.

Libowitzky E (1999) Correlation of O-H Stretching Frequencies and O-H· · ·O Hydrogen Bond Lengths in Minerals. *Monatshefte fiir Chemie*, 130, 1047–1059.

London D. (2008) Pegmatites. *The Canadian Mineralogist, Special Publication,* 10. Pp. 1–347.

London D. (2014) A petrologic assessment of internal zonation in granitic pegmatites. *Lithos*, 184-187, 74–104.

London D. and Evensen M.J. (2002) Beryllium in silicic magmas and the origin of beryl-bearing pegmatites. Pp. 445–486 in: *Beryllium – mineralogy, petrology and geochemistry* (E.S. Grew, editor). *Reviews in Mineralogy and Geochemistry,* 50. Mineralogical Society of America, Washington DC.

Markl G. and Schumacher J. (1997) Beryl stability in local hydrothermal and chemical environments in a mineralized granite. *American Mineralogist,* 82, 195–203.

Martin R. F. and De Vito C. D. (2014) The late-stage miniflood of Ca in granitic pegmatites: an open-system acid-reflux model involving plagioclase in the exocontact. *The Canadian Mineralogist,* 52, 165–181.

Melleton J., Gloaguen E., Frei D., Novák M. and Breiter K. (2012) How are the time of emplacement of rare-element pegmatites, regional metamorphism and magmatism interrelated

in the Moldanubian Domain of Variscan Bohemian Massif, Czech Republic. *The Canadian Mineralogist*, 50, 1751–1773.

Merlet C. (1994) An Accurate Computer Correction Program for Quantitative Electron Probe Microanalysis. *Microchimical Acta*, 114/115, 363–376.

Němec D. (1990) Neues zur Mineralogie eines Hambergit-führenden Pegmatitgangs von Kracovice (bei Třebíč, Westmorava, ČSFR). *Zeitschrift Geologische Wissenschaften*, 18, 1105–1115.

Novák M. (1998) Fibrous blue dravite; an indicator of fluid composition during subsolidus replacement processes in Li-poor granitic pegmatites in the Moldanubicum, Czech Republic. Journal of Geosciences 43, 24–30.

Novák M. and Cempírek J. (2010) Granitic pegmatites and mineralogical museums in the Czech Republic. IMA2010. Field trip guide CZ2. *Acta Mineralogica-Petrographica, Field guide series,* 6, 1–56.

Novák M. and Filip J. (2010) Unusual (Na,Mg)-enriched beryl and its breakdown products (beryl II, bazzite, bavenite) from euxenite-type NYF pegmatite related to the orogenic ultrapotassic Třebíč Pluton, Czech Republic. *The Canadian Mineralogist*, 48, 615–628.

Novák M., Korbel P. and Odehnal F. (1991) Pseudomorphs of bertrandite and epididymite after beryl from Věžná, Western Moravia, Czechoslovakia. *Neues Jahrbuch für Mineralogie, Monatshefte*, 473–480.

Novák M., Černý P., Kimbrough D. L., Taylor M. C. and Ercit, T. S. (1998) U-Pb ages of monazite from granitic pegmatites in the Moldanubian Zone and their geological implications. *Acta Universitatis Carolinae, Geologica*, 42, 309–310.

Novák M., Škoda R., Gadas P., Krmíček L. and Černý P. (2012) Contrasting origins of the mixed (NYF+LCT) signature in granitic pegmatites, with examples from the Moldanubian Zone, Czech Republic. *The Canadian Mineralogist*, 50, 1077–1094.

Novák M., Kadlec T. and Gadas P. (2013) Geological position, mineral assemblages and contamination of granitic pegmatites in the Moldanubian Zone, Czech Republic; examples from the Vlastějovice region. *Journal of Geosciences,* 58, 21–47.

Novák M., Gadas P., Cempírek J., Škoda R., Breiter K., Kadlec T., Loun J. and Toman J. (2015a) B1 Granitic pegmatites of the Moldanubian Zone, Czech Republic. In PEG 2015: 7th International Symposium on Granitic Pegmatites, Field trip guidebook, 23–72.

Novák M., Čopjaková R., Dosbaba M., Galiová M.V., Všianský D. and Staněk J. (2015b) Two paragenetic types of cookeite from the Dolní Bory-Hatě pegmatites, Moldanubian Zone, Czech Republic: Proximal and distal alteration products of Li-bearing sekaninaite. *The Canadian Mineralogist*, 53(6), 1035–1048.

Novák M., Prokop J., Losos Z. and Macek I. (2017) Tourmaline, an indicator of external Mg-contamination of granitic pegmatites from host serpentinite; examples from the Moldanubian Zone, Czech Republic. *Mineralogy and Petrology*, 111, 625–641.

Novák M., Dolníček Z., Zachař A., Gadas P., Nepejchal M., Sobek K., Škoda R. and Vrtiška L. (2023a) Mineral assemblages and compositional variations in bavenite–bohseite from granitic pegmatites of the Bohemian Massif, Czech Republic. *Mineralogical Magazine*, 87, 415–432.

Novák M., Toman J., Škoda R., Šikola D. and Mazuch, J. (2023b) Review of zeolite mineralizations from the high-grade metamorphosed Strazek Unit, Moldanubian Zone, Czech Republic. *Journal of Geosciences*, 68(2), 111–138.

Novotný F. and Cempírek J. (2021) Mineralogy of the elbaite-subtype pegmatite from Dolní Rožínka. *Acta Musei Moraviae, Scientiae Geologicae*, 1, 1–33 (in Czech with English summary).

Palinkaš S.S., Wegner R., Čobić A., Palinkaš L.A., Barreto S.D.B., Váczi T. and Bermanec, V. (2014) The role of magmatic and hydrothermal processes in the evolution of Be-bearing pegmatites: Evidence from beryl and its breakdown products. *American Mineralogist*, 99(2-3), 424–432.

Passaglia E. (1970) The crystal chemistry of chabazites. *American Mineralogist*, 55(7-8), 1278–1301.

Pauliš P. and Cempírek J. (1998) Harmotome and chabazite from desilicated pegmatite in Věžná near Bystřice nad Pernštejnem. Vlastivěd Sborník Vysočiny, Oddělení Vědy přírodní, 13, 349–350 (in Czech).

Perrotta A. J. (1976) A low-temperature synthesis of a harmotome-type zeolite. *American Mineralogist*, 61(5-6), 495–496.

Pertoldová J., Týcová P., Verner K., Košuličová M., Pertold Z., Košler J., Konopásek J. and Pudilová M. (2009) Metamorphic history of skarns, origin of their protolith and implications

for genetic interpretation; an example from three units of the Bohemian Massif. *Journal of Geosciences*, 54(2), 101–134.

Pertoldová J., Verner K., Vrána S., Buriánek D., Štědrá V. and Vondrovic L. (2010) Comparison of lithology and tectonometamorphic evolution of units at the northern margin of the Moldanubian Zone: implications for geodynamic evolution in the northeastern part of the Bohemian Massif. *Journal of Geosciences*, 55(4), 299–319.

Pieczka A., Szuskiewicz A., Szełeg E. and Nejbert K. (2019) Calcium minerals and late stage metasomatism in the Julianna pegmatitic system, the Góry Sowie Block, SW Poland. Contributions to the 9th international Symposium PEG 2019, 56–58.

Přikryl J., Novák M. and Gadas P. (2012) Compositional variations in Cs,Mg,Fe-enriched beryl from common pegmatite in Kovářová, Svratka Unit, Czech Republic. *Acta Mineralogica-Petrographica, Abstract Series,* Szeged 7, 112.

Přikryl J., Novák M., Filip J., Gadas P. and Galiová M. V. (2014) Iron+Magnesium-bearing beryl from granitic pegmatites: An EMPA, LA-ICP-MS, Mössbauer spectroscopy, and powder XRD study. *The Canadian Mineralogist*, 52, 271–284.

Rybnikova O., Uher P., Novák M., Chládek Š., Bačík P., Kurylo S., and Vaculovič T. (2023) Chrysoberyl and associated beryllium minerals resulting from metamorphic overprinting of the Maršíkov–Schinderhübel III pegmatite, Czech Republic. *Mineralogical Magazine*, 87, 369–381.

Schulmann K., Lexa O., Janoušek V., Lardeaux J. M. and Edel J.B. (2014) Anatomy of a diffuse cryptic suture zone: An example from the Bohemian Massif, European Variscides. *Geology*, 42(4), 275–278.

Schulz B., Sandmann D. and Gilbricht S. (2020) SEM-Based Automated Mineralogy and Its Application in Geo- and Material Sciences. *Minerals*, 10(11),1004. doi: 10.3390/min10111004

Sharma K. S., Yoder S. H. Jr. and Matson W. D. (1988) Raman study of some melilites in crystalline and glassy states. *Geochimica et Cosmochimica Acta*, 52(8), 1961–1967. doi: 10.1016/0016-7037(88)90177-9

Sejkora J., Pauliš P., Dolníček Z., Plášil J. and Škoda R. (2023) Zeolites from the quarry Bernartice in near Zruč nad Sázavou (Czech Republic). *Acta Musei Moraviae, Scientiae geologicae*, 108 (2), 171–193 (with English summary).

Sojka A. (1969) *Mineralogical and textural/paragenetic relations in pegmatites from ore-deposit Olší*. Unpublished Ms thesis, Masaryk University, Brno. Pp. 1–76 (in Czech)

Štípská P., Powell R., Hacker B. R., Holder R. and Kylander-Clark, A. R. C. (2016) Uncoupled U/Pb and REE response in zircon during the transformation of eclogite to mafic and intermediate granulite (Blanský les, Bohemian Massif). *Journal of Metamorphic Geology*, 34(6), 551–572.

Tajčmanová L., Konopásek J. and Schlumann K. (2006) Thermal evolution of the orogenic lower crust during exhumation within a thickened moldanubian root of the variscan belt of central europe. *Journal of Metamorphic Geology*, 24 (2), 119–134. https://doi.org/ 10.1111/j.1525-1314.2006.00629.x.

Teertstra D. K., Černý P. and Novák M. (1995) Compositional and textural evolution of pollucite in rare-element pegmatites of the Moldanubicum. *Mineralogy and Petrology*, 55, 37–52.

Thomas R. and Davidson P. (2012) Water in granite and pegmatite-forming melts. *Ore Geology Reviews*, 46, 32–46.

Thomas R., Davidson P., Rhede D. and Leh M. (2009). The miarolitic pegmatites from the Königshain: a contribution to understanding the genesis of pegmatites. *Contributions to Mineralogy and Petrology*, 157, 505–523.

Toman J. and Novák M. (2018) Textural relations and chemical composition of minerals from a pollucite + harmotome + chabazite nodule in the Věžná I pegmatite, Czech Republic. *The Canadian Mineralogist*, 56(4), 375–392.

Toman J. and Novák M. (2020) Beryl-columbite pegmatite Věžná I. *Acta Musei Moraviae, Scientiae Geologicae*, 107, 3–42. (in Czech with English summary)

Uher P., Chudík P., Bačík P., Vaculovič T. and Galiová M. (2010) Beryl composition and evolution trends: an example from granitic pegmatites of the beryl-columbite subtype Western Carpathians Slovakia. *Journal of Geosciences*, 55, 69–80.

Uher P., Ozdín D., Bačík P., Števko M., Ondrejka M., Rybnikova O., Chládek Š., Fridrichová J., Pršek J. and Puškelová Ľ. (2022) Phenakite and bertrandite: products of post-magmatic alteration of beryl in granitic pegmatites (Tatric Superunit, Western Carpathians, Slovakia). *Mineralogical Magazine*, 86, 715–729.

Veksler I. V. and Thomas R. (2002) An experimental study of B-, P- and F- rich synthetic granite pegmatite at 0.1 and 0.2 GPa. *Contributions to Mineralogy and Petrology*, 143, 673–683.

Verner K., Buriánek D., Vrána S., Vondrovic L., Pertoldová J., Hanžl P. and Nahodilová R. (2009) Tectonometamorphic features of geological units along the northern periphery of the Moldanubian Zone. *Journal of Geosciences*, 54(2), 87–100.

Wang R. C., Che X. D., Zhang W. L., Zhang A. C. and Zhang H. (2009) Geochemical evolution and late re-equilibration of Na–Cs-rich beryl from the Koktokay #3 pegmatite (Altai, NW China). *European Journal of Mineralogy*, 21, 795–809.

Wang X. and Li J. (2020) In situ observations of the transition between beryl and phenakite in aqueous solutions using a hydrothermal diamond-anvil cell. *The Canadian Mineralogist*, 58(6), 803–814.

Warr L.N. (2021) IMA–CNMNC approved mineral symbols. *Mineralogical Magazine*, 85(3), 291–320.

Weisenberger T. and Bucher K. (2010) Zeolites in fissures of granites and gneisses of the Central Alps. *Journal of Metamorphic Geology*, 28(8), 825–847.

Weisenberger T. and Bucher K. (2011) Mass transfer and porosity evolution during low temperature water–rock interaction in gneisses of the Simano nappe: Arvigo, Val Calanca, Swiss Alps. *Contributions to Mineralogy and Petrology*, 162(1), 61–81.

Wertich V., Kubeš M., Leichmann J., Holá M., Haifler J., Mozola J., Hršelová P. and Jaroš M. (2022) Trace element signatures of uraninite controlled by fluid-rock interactions: A case study from the Eastern Moldanubicum (Bohemian Massif). *Journal of Geochemical Exploration*, 243, 107111.

Wise M. A., Müller A. and Simmons W. B. (2022) A proposed new mineralogical classification system for granitic pegmatites. *The Canadian Mineralogist*, 60(2), 229–248.

Wood S.A. (1992) Theoretical prediction of speciation and solubility of beryllium in hydrothermal solution to 300° C at saturated vapor pressure: Application to bertrandite/phenakite deposits. *Ore Geology Reviews*, 7(4), 249–278.

Zachař A., Novák M. and Škoda R. (2020) Beryllium minerals as monitors of geochemical evolution from magmatic to hydrothermal stage; examples from NYF pegmatites of the Třebíč Pluton, Czech Republic. *Journal of Geosciences*, 65(3), 153–172.

Figure captions

Fig. 1. Simplified geological map of the northeastern part of the Bohemian Massif including Moldanubian Zone and Svratka Crystalline Unit.

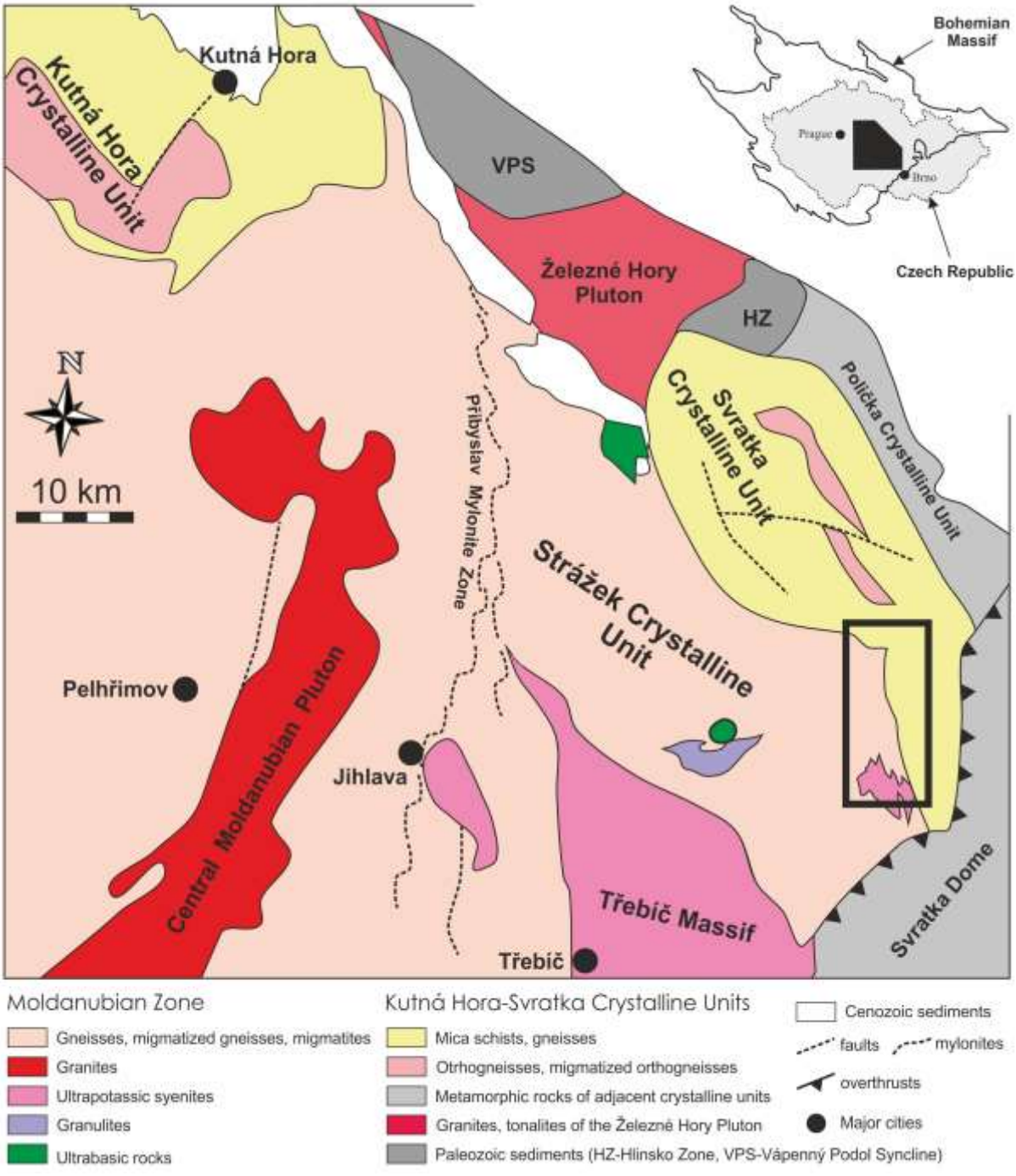

Fig. 2. Simplified geological map of the Rožná-Olší ore field with the examined pegmatites.

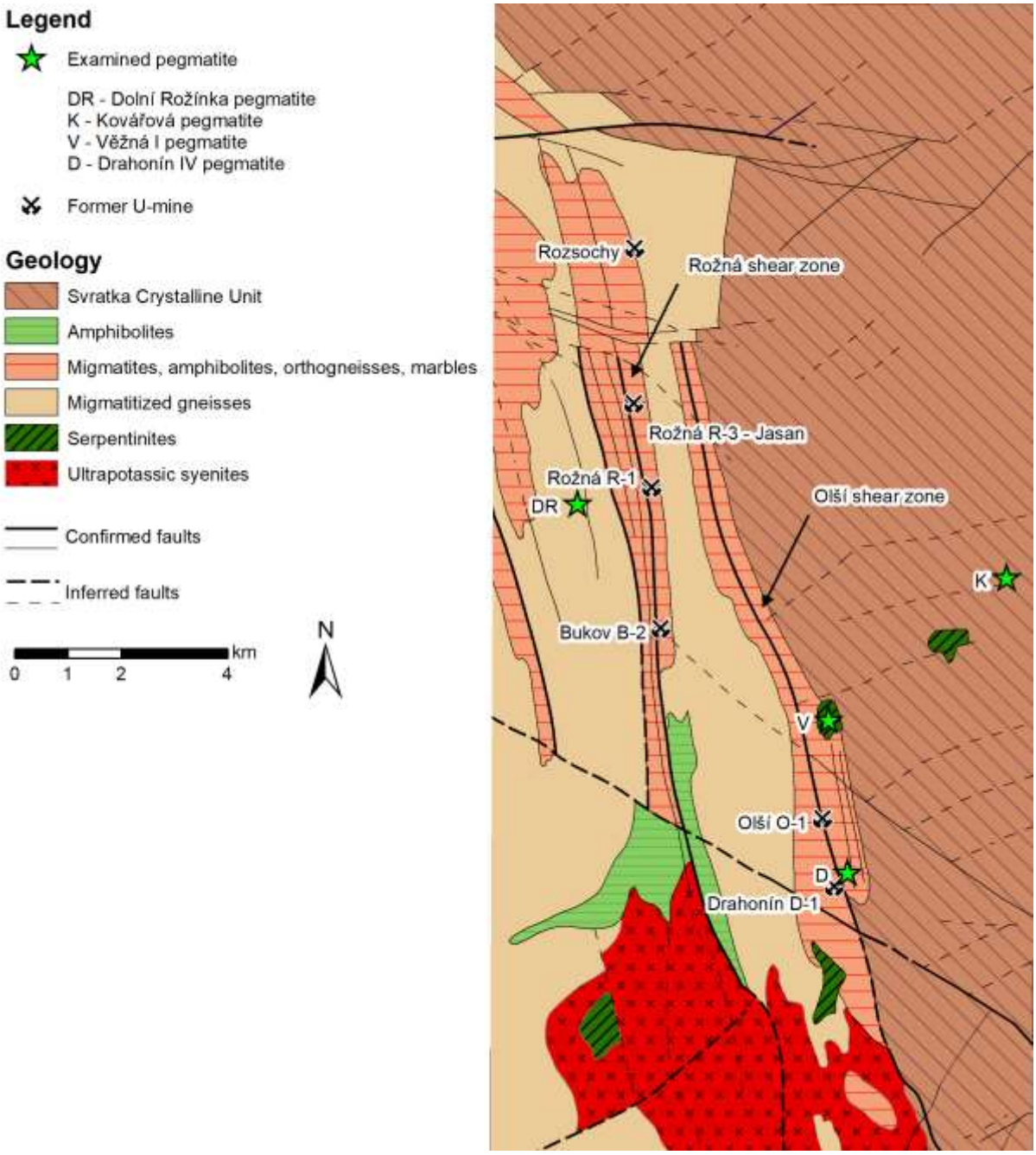

Fig. 3. Idealized cross-section of the Drahonín IV pegmatite (modified from Sojka, 1969)

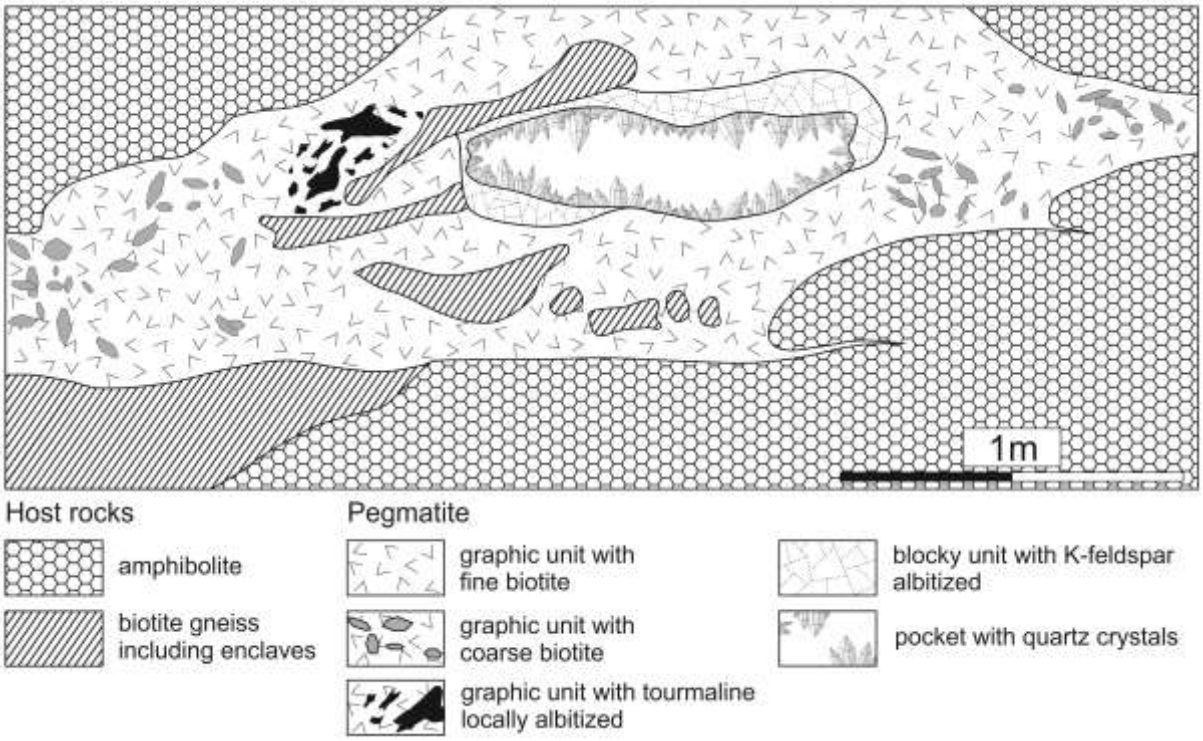

Fig. 4. Idealized cross-section of the Věžná I pegmatite (modified from Černý and Povondra, 1967).

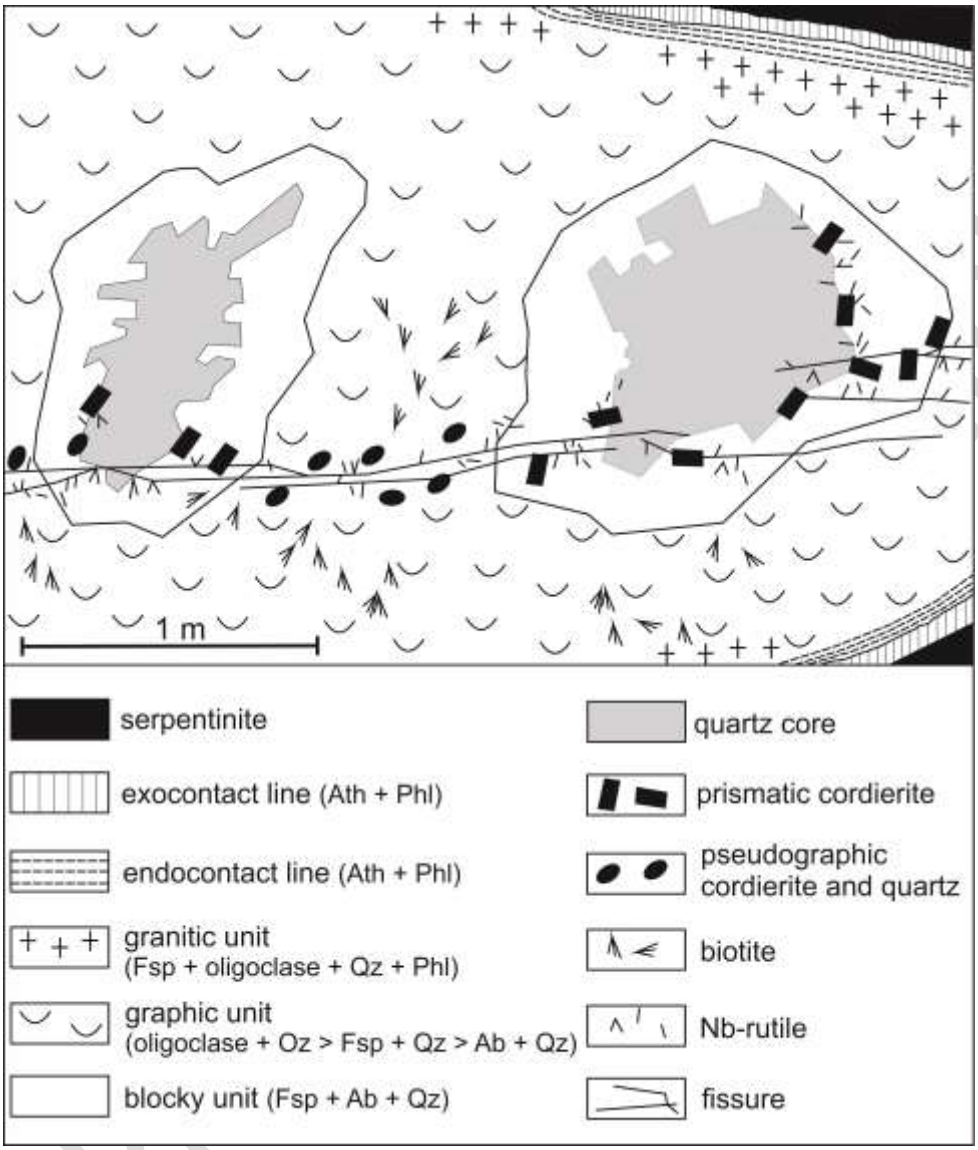

Fig. 5. BSE images of primary and secondary beryl; (a) relics of homogeneous primary beryl II, Drahonín IV; (b) homogeneous primary beryl II with veinlet of heterogeneous secondary Cs-enriched beryl IIA, Věžná I; (c) primary beryl IV with numerous veinlets of heterogeneous secondary beryl IVA (Cs-rich beryl to pezzottaite), Dolní Rožínka, CM – clay minerals; (d) prismatic zoned crystal of primary beryl I with narrow rims of beryl IA, Kovářová. Scale bar for all figures 200 µm. Used abbreviations according to Warr (2021) in Figs. 5, 7, 8 and 10: Ab – albite, Apy – arzenopyrite, Bvn – bavenite, Brl – beryl, Btd – bertrandite, Cst – cassiterite, Chl – chlorite, Edd – epidydimite, Grt – garnet, Hgug – hydroxylgugiaite, Hrm – harmotome, Kfs – K-feldspar, Lö – löllingite, Mil – milarite, Ms – muscovite, Py – pyrite, Qz – quartz, Tur – tourmaline,

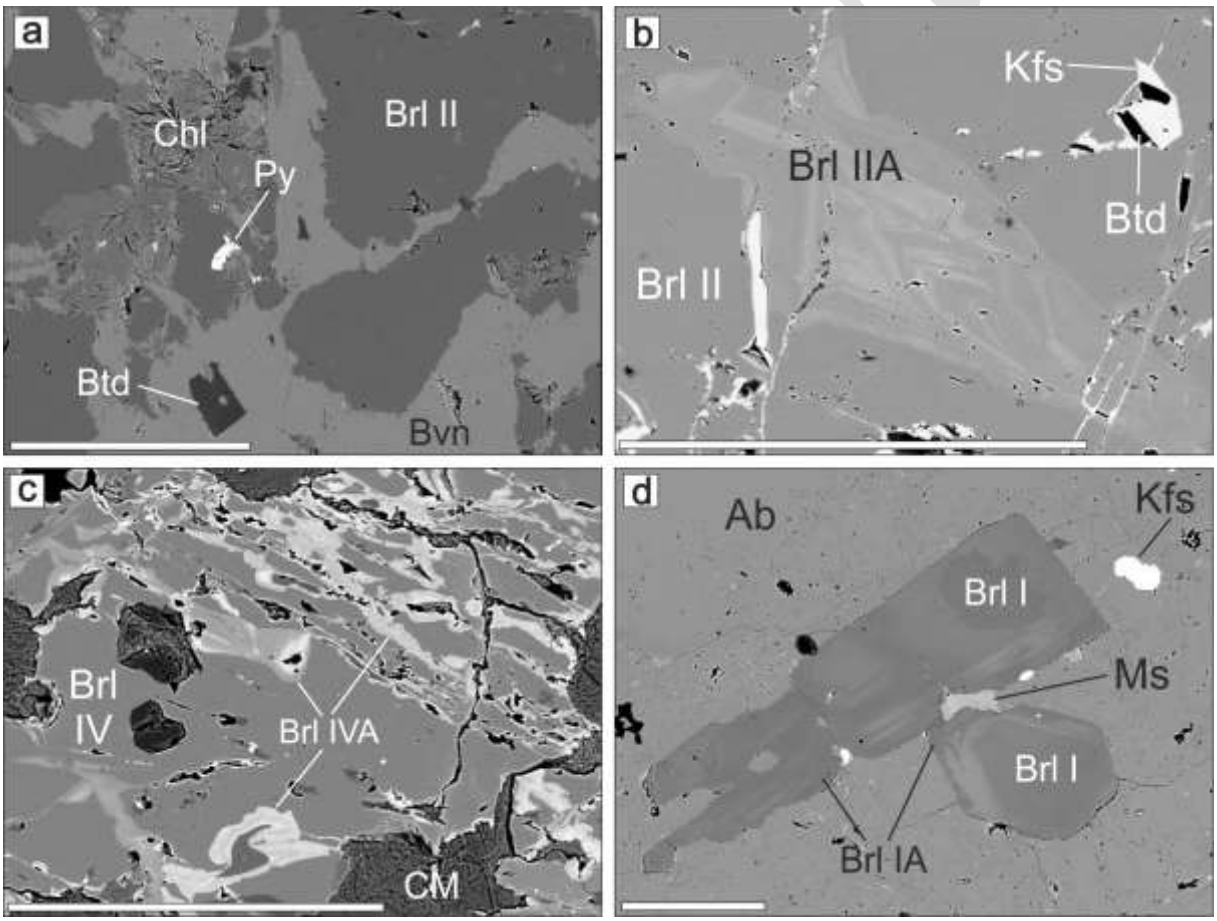

Fig. 6. Classification diagrams for primary and secondary beryl from (a), (b) the examined pegmatites Drahonín IV, Věžná I and Kovářová and (c), (d) from Dolní Rožínka (slightly modified from Novotný and Cempírek, 2021).

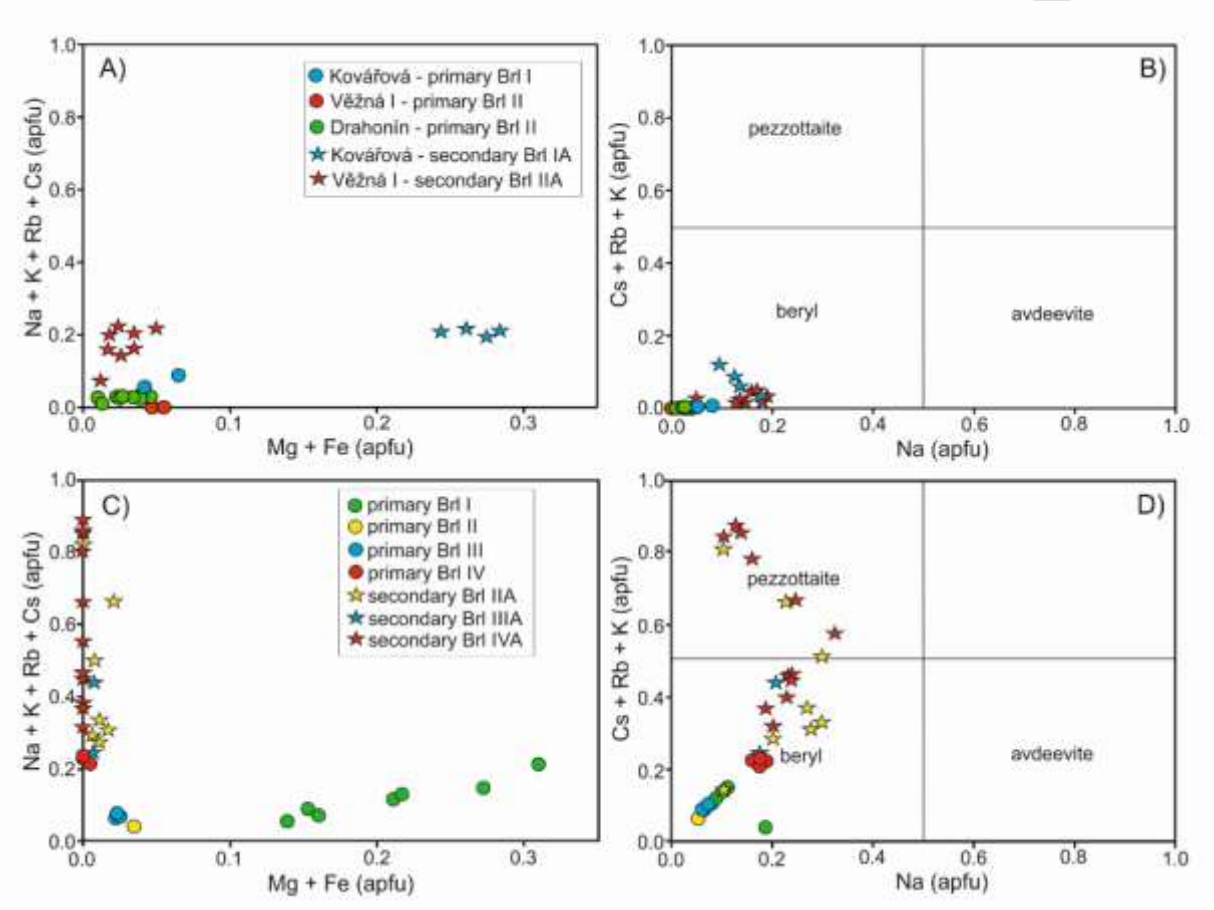

Fig. 7. BSE images of assemblages of secondary Be-minerals from the Drahonín IV pegmatite.

(a), (b) bertrandite crystals enclosed in bavenite from pseudomorph after beryl I (D-i); (c) bavenite + chlorite after beryl I (D-i) with inclusion of cassiterite; (d) contact of garnet replaced by muscovite + chlorite and beryl II replaced by bavenite-bohseite, less common euhedral bertrandite, and pyrite (D-ii); (e) bertrandite + bavenite + K-feldspar + chlorite after beryl II (D-ii); (f) heterogeneous milarite + quartz + albite in veinlet cutting beryl II (D-iv). Scale bar for all figures 200 µm.

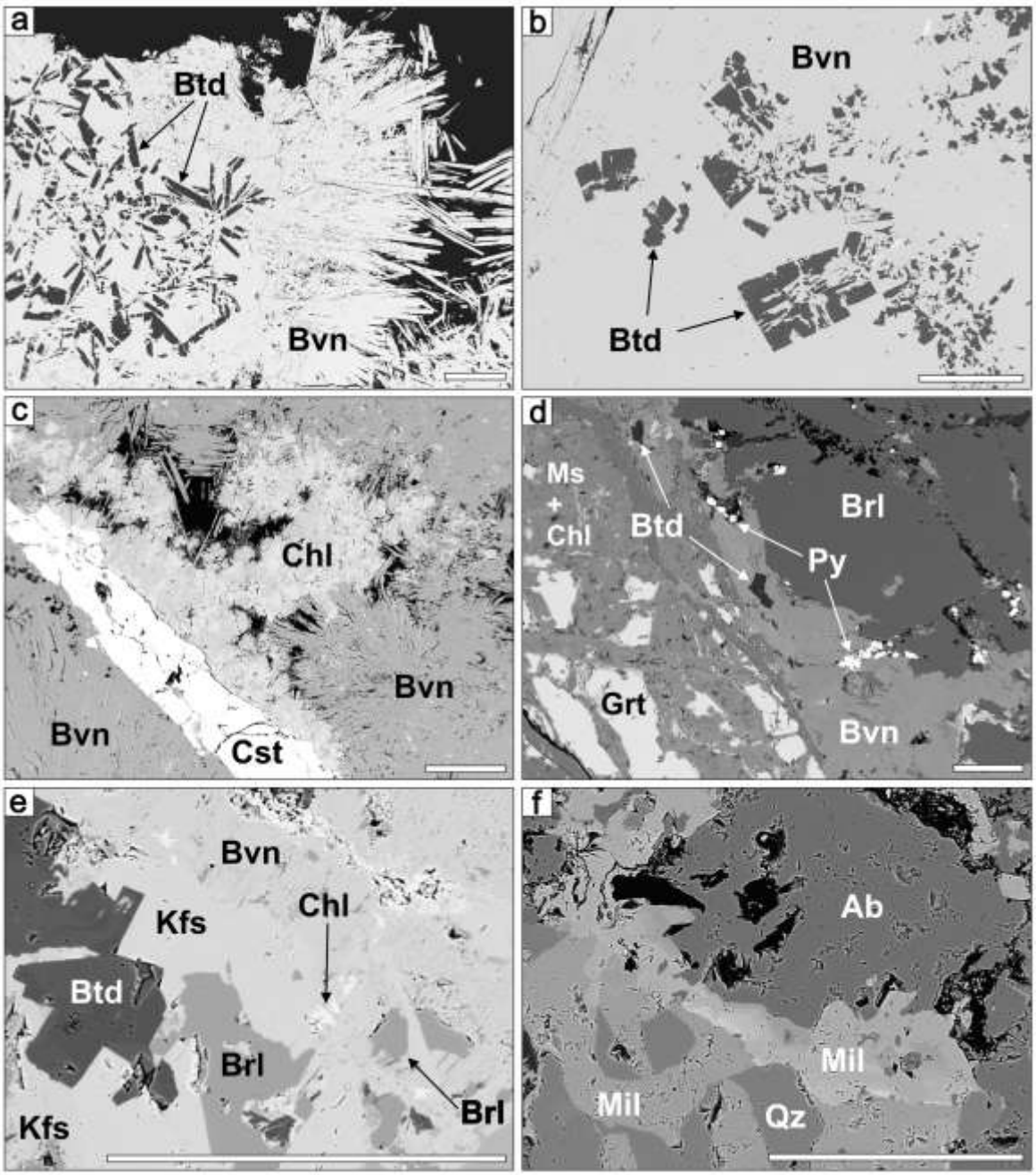

Fig. 8. BSE images of assemblages of secondary Be-minerals from the Věžná I pegmatite.

(a) K-feldspar (locally Ba-enriched) + bertrandite + harmotome after beryl II (V-i); (b) the assemblage (V-i) K-feldspar + bertrandite with euhedral grain of löllingite+arsenopyrite is cutting by thin epidydimite veinlet (V-ii); (c) the assemblage (V-i) cut by epidydimite veinlet (V-ii); (d) contact of zoned tourmaline and beryl II, the assemblage (V-i) is developed exclusively within the beryl grain; (e) the assemblage (V-i) with abundant bertrandite + harmotome is cut by epidydimite veinlets (V-ii); (f) veinlets of early assemblages (V-i) and (V-ii) cut by veinlet of the assemblage (V-iii) hydroxylgugiaite + K-feldspar (both minerals are not recognizable in this BSE image). Scale bar for all figures 200 µm.

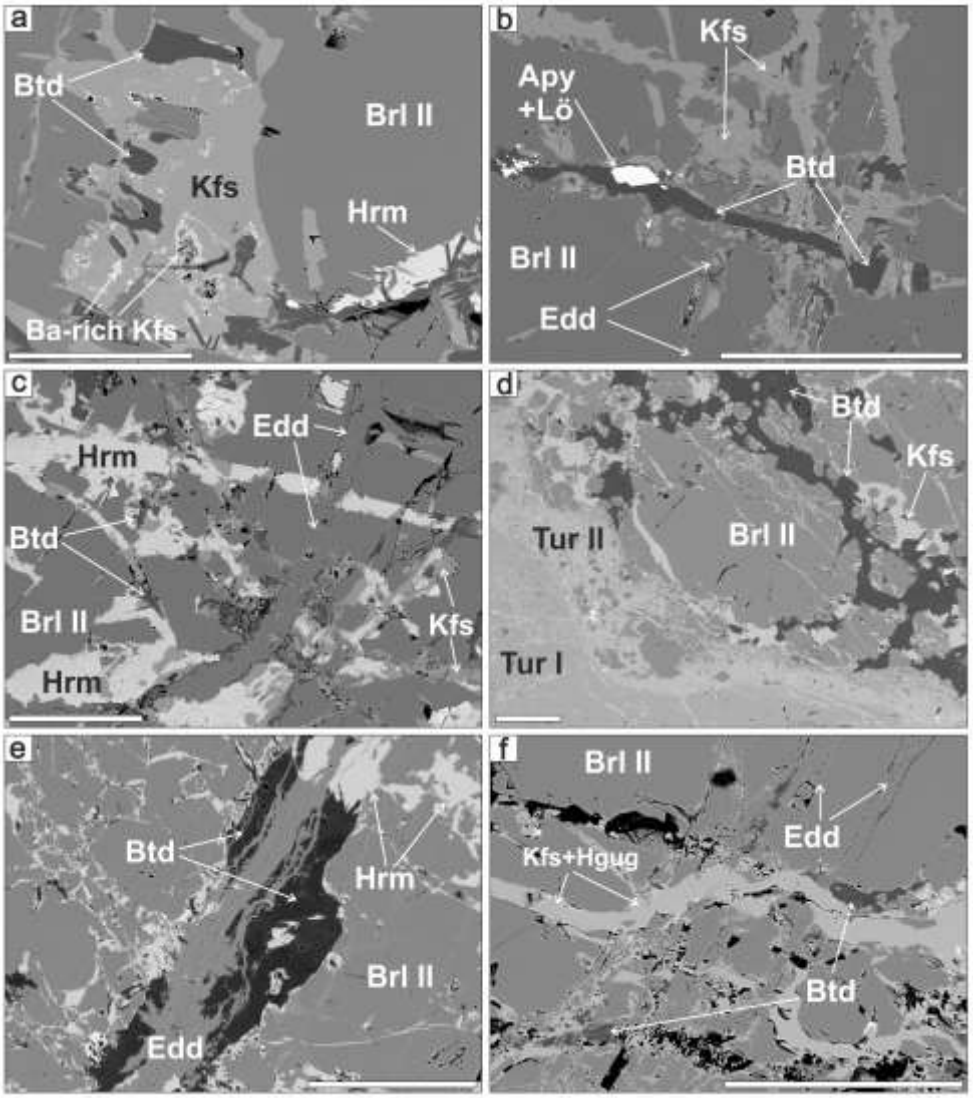

Fig. 9. Raman spectra of selected secondary minerals.

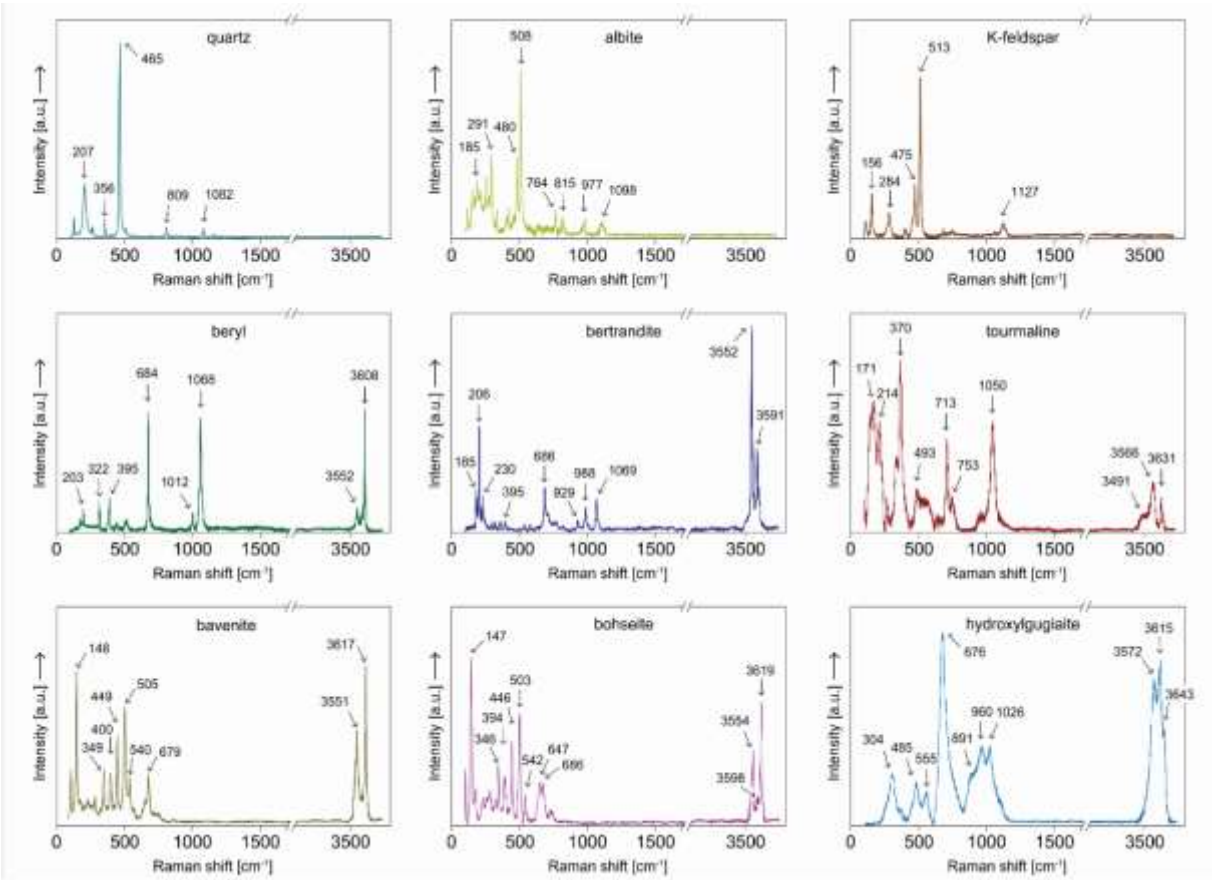

Fig. 10. Representative comparison between BSE and optical microscope images of hydroxylgugiaite. (a) BSE image shows the merging of colour intensities for hydroxylgugiaite and K-feldspar, making it seem like one phase; (b) On the contrary, these phases can be easily distinguished on reflected light microscopy.

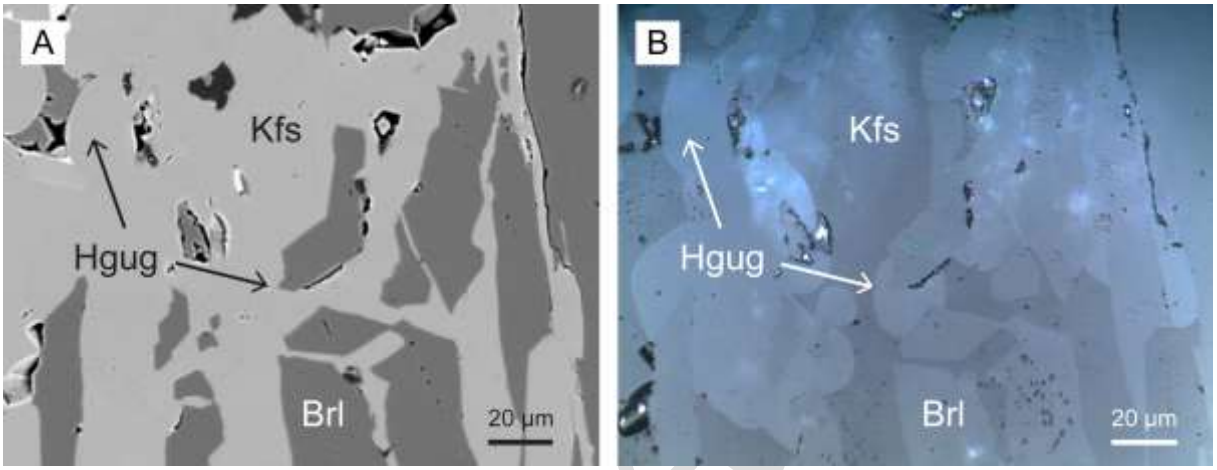

Fig. 11. Assemblage stability diagram in the Be-Al-Si-O-H system at *P* = 100 MPa (modified from Barton, 1986, Barton and Young, 2002). Note very small stability field of the assemblage bertrandite + K-feldspar. Used abbreviations according to Warr (2021): Brl – beryl, Btd – bertrandite, Esc – euclase, Kfs – K-feldspar, Ms – muscovite, Phk – phenakite, Qz – quartz, W – water.

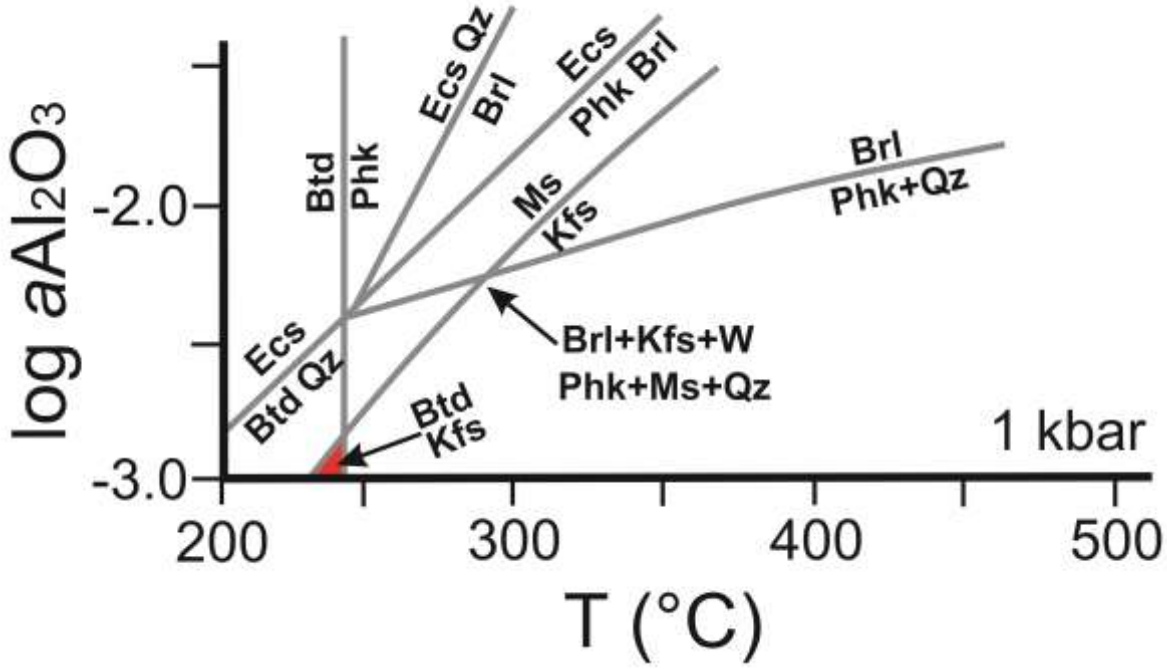

Table captions

Table 1. Geological setting and mineral assemblages of the examined granitic pegmatites.

Table 1

	Geological setting			Minor minerals						Selected accessory minerals	Significant alterations	Source
locality / pegmatite subtype	thickness(m) /strike/dip	host rock / contact	miarolitic pockets	Bt	Ms	Tur	Grt	Crd	Brl			
Drahonín IV / beryl-columbite subtype	3/E-W/50°N	amphibolite, gneiss / discordant	abundant	A	M	A	R		M	Fap, Sps, Srl, Cal, Py, Cst	Kfs → Ab, Kfs → Ms, Sps → Ms, Chl	1, this work
Věžná I / beryl-columbite to elbaite subtype	3/NW-SE/80°SN	serpentinite / discordant	rare	A	M	A		A	R	Fap, Drv, Srl, Nb-rutile, Clb, Mnz-Ce, Xtm-Y, Zrn, Cst, Tpz, Trl, Elb, Pol, Hrm, Pln, Sok	Qz → kerolite; Phl → Vrm; Crd → Drv; Crd → Ms, Chl, Phl, Brl, Prg; Crd → Ms, Aeg, Arf, Edd, Prg; Tur → Kfs, Arf, Ttn	2, 3, 4, 5, 6, 7, 8, 9, this work
Dolní Rožínka / elbaite subtype	1.3/N-S/70-85°E	dolomite marble, amphibolite / discordant	common	A		A	A		R	Fap, Sps, Clb, Cst, Mnz-Ce, Zrn, Srl, Elb, Pol, Pln, Sok	Bt → Tur; Tur → Tur; Tur → Plg	10
Kovářová / beryl-columbite subtype	~0.5m fragments	amphibolite / concordant	absent	R	A	R	R		R	Fap, Alm, Ilm, Srl, Mnz-Ce, Xtm-Y, Zrn	Kfs → Ab, Kfs → Ms	11, 12

A -
abundant
M - minor
R - rare

1 – Sojka 1969, 2 – Černý 1965, 3 – Černý and Miškovský 1966, 4 – Novák 1998, 5 – Dosbaba and Novák 2012, 6 - Gadas et al. 2020, 7 – Novák et al. 2017, 8 – Toman and Novák 2020, 9 – Čopjaková et al. 2021, 10 – Novotný and Cempírek 2021, 11 – Přikryl et al. 2012, 12 – Přikryl et al. 2014.

Used abbreviations according to Warr (2021): Ab – albite, Aeg – aegirine, Alm – almandine, Arf – arfvedsonite, Brl – beryl, Bt – biotite, Cal – calcite, Cst – cassiterite, Clb – columbite, Chl – chlorite, Crd – cordierite, Drv – dravite, Edd – epidydimite, Elb – elbaite, Fap – fluorapatite, Hrm – harmotome, Ilm – ilmenite, Kfs – K-feldspar, Mnz-Ce – monazite-(Ce), Ms – muscovite, Phl – phlogopite, Plg – plagioclase, Pln – polylithionite, Pol – pollucite, Prg – pargasite, Py – pyrite, Qz – quartz, Sok – sokolovaite, Sps – spessartine, Srl – schorl, Tpz – topaz, Trl – triplite, Ttn – titanite, Tur – tourmaline, Vrm – vermiculite, Xtm-Y – xenotime-(Y), Zrn – zircon.

Table 2. Review of the published data about beryl and secondary Be-minerals from the Drahonín IV, Věžná I, Dolní Rožínka and Kovářová pegmatites.

Table 2

		Proximal secondary minerals			
locality / source	primary beryl	secondary beryl / abundance	other Be-minerals	associated minerals	degree of alteration
Drahonín IV, Sojka 1969	beryl I	not found	bavenite	chlorite	extreme
	beryl II	not found	none		strong
Věžná I, Novák et al. 1991, Toman and Novák 2020	beryl I	not found	none		none
	beryl II	not found	epidydimite, bertrandite	K-feldspar, muscovite	strong
	beryl III	not found	none		none
Dolní Rožínka, Novotný and Cempírek 2021	beryl I	none	none		none
	beryl II	Cs-rich beryl / M	none		weak
	beryl III	Cs-rich beryl / M	none		weak
	beryl IV	Cs-rich beryl to pezzottaite / A	none		weak

	beryl IV	not found	bertrandite	none	almost total
Kovářová, Přikryl et al. 2012, 2014	beryl I	beryl / R	none	none	none
	beryl II	beryl / A	none	Cs-annite, muscovite	moderate
	beryl III	not found	none	none	none

A - abundant
M - minor
R - rare

Table 3. Representative compositions of primary and secondary beryl.

Locality	Věžná I		Drahonín IV			Kovářová		
Mineralization	Brl II	Brl IIA	Brl II			Brl I	Brl I	Brl IA
	primary	secondary	primary			primary	primary	secondary
Sample	11	1	35	4d	92	6	26	32
SiO_2	68.51	67.38	67.51	66.75	68.41	65.89	65.61	67.14
Al_2O_3	18.01	17.58	18.30	18.11	18.43	15.02	15.54	16.56
BeO*	13.30	13.95	13.97	13.83	14.15	13.64	13.53	13.88
FeO	0.24	0.23	0.31	0.52	0.34	2.02	1.53	0.86
MgO	0.21	0.24	bdl	bdl	0.01	1.75	1.04	1.01
Na_2O	bdl	0.96	0.17	0.14	0.15	1.19	0.66	0.83
K_2O	bdl	bdl	bdl	bdl	0.03	bdl	bdl	0.16
Rb_2O	bdl	bdl	bdl	bdl	bdl	0.08	0.11	0.10
Cs_2O	bdl	1.25	bdl	bdl	bdl	0.31	1.45	0.08
∑ oxide	101.07	101.59	100.26	99.35	101.52	99.90	99.47	100.62
Si	6.067	6.031	6.035	6.028	6.039	6.031	6.056	6.040
Al	1.880	1.885	1.928	1.928	1.918	1.620	1.691	1.756
Be	3.000	3.000	3.000	3.000	3.000	3.000	3.000	3.000
Fe	0.018	0.017	0.023	0.039	0.025	0.155	0.118	0.065
Mg	0.028	0.032	—	—	0.001	0.239	0.143	0.135
Na	—	0.167	0.029	0.025	0.026	0.211	0.118	0.145
K	—	—	—	—	0.003	—	—	0.018
Rb	—	—	—	—	—	0.004	0.006	0.006
Cs	—	0.048	—	—	—	0.012	0.057	0.003
∑ cat	10.993	11.149	11.016	11.020	11.017	11.272	11.188	11.168
O	18	18	18	18	18	18	18	18

Note: contents on a basis of 18 O; *determined by stoichiometry; bdl = below detection limit

Table 4. Review of secondary mineral assemblages and their geochemical signature.

Table 4

Locality	**Beryl**		**Secondary assemblages**			**Geochemical signature except secondary beryl**									
	Primary	Secondary	assemblage / abundance	Be-minerals	other associated minerals	Be	Ca	Na	K	Ba	Pb	Zn	Fe	S	As	
Drahonín IV	beryl I	not found	(D-i) / A	Bvn-Bhs > Btd	Chl, Sp, Py > Gn, Sn-Ttn, Sks	A	A				R	R	R	R		Be, Ca
	beryl II	not found	(D-ii) / R	Bvn-Bhs > Btd	Anl, Gis, Chl > Lmt, Slc, Py	A	A	M					R	R		Be, Ca > Na
			(D-iii) / R	Btd >> Hgug	Kfs	A			A							Be, K
			(D-iv) / VR	Mil > Bvn-Bhs	Kfs, Qz, Ms, Chl	A	A		A							Ca, K, Be
																Be, Ca > K, Na
Věžná I	beryl II	common	(V-i) / A	Btd	Kfs > Hrm, Brt, Apy, Lö	A			A	M			R	R	R	Be, K > Ba
			(V-ii) / M	Edd > Hgug	Heu, Brt, Hrm	A	A	A		R				R		Be, Na,Ca > Ba
			(V-iii) / M	Hgug	Kfs	A	A		A							K, Be, Ca
																Be, K > Ca, Ba, Na
Dolní Rožínka	beryl IV	common	VR	Btd	none	A									R	**Be**
Kovářová	beryl I	common		none												

A - abundant

M -

minor
R - rare
VR - very rare

Used abbreviations according to Warr (2021): Anl – analcime, Apy – arzenopyrite, Bvn – bavenite, Bhs – bohseite, Brt – baryte, Btd – bertrandite, Chl – chlorite, Edd – epidydimite, Gis – gismondine, Gn – galena, Heu – heulandite, Hgug – hydroxylgugiaite, Hrm – harmotome, Kfs – K-feldspar, Lmt – laumontite, Lö – löllingite, Mil – milarite, Ms – muscovite, Py – pyrite, Qz – quartz, Sks – stokesite, Slc – scolecite, Sp – sphalerite, Ttn – titanite,

Table 5. Representative compositions of secondary Be-minerals.

Locality	Věžná I				Drahonín IV					
Mineralization	epididymite		hydroxylgugiaite		bavenite			milarite		
Sample	13	14	24	25	4	95	97	1	19	20
SiO_2	75.26	75.62	46.05	46.11	58.17	60.20	59.93	69.22	71.86	72.35
Al_2O_3	0.54	0.66	0.58	0.68	8.13	5.35	5.57	2.39	2.35	3.93
Y_2O_3	bdl	bdl	bdl	bdl	bdl	bdl	bdl	4.83	bdl	bdl
BeO*	10.44	10.52	12.70	12.75	6.32	7.15	7.16	4.52	5.00	5.06
FeO	bdl	bdl	0.27	0.21	bdl	0.03	0.04	bdl	bdl	bdl
MnO	bdl	bdl	bdl	bdl	bdl	0.05	0.04	bdl	bdl	bdl
MgO	bdl	bdl	bdl	0.16	bdl	0.01	bdl	bdl	bdl	bdl
SrO	0.28	bdl	bdl	bdl	bdl	bdl	bdl	bdl	bdl	bdl
BaO	bdl	bdl	bdl	bdl	bdl	0.04	0.01	bdl	bdl	bdl
Cs_2O	bdl	bdl	bdl	bdl	bdl	bdl	0.03	bdl	bdl	bdl
Rb_2O	bdl	0.22	bdl	bdl	bdl	bdl	bdl	bdl	bdl	bdl
CaO	0.29	0.15	33.59	33.65	24.58	24.59	24.81	7.82	11.62	11.72
Na_2O	11.29	11.86	1.10	1.05	bdl	0.25	0.22	0.31	0.68	0.34
K_2O	0.20	0.21	bdl	bdl	bdl	0.03	bdl	4.62	5.96	5.46
P_2O_5	bdl	bdl	bdl	bdl	bdl	0.02	0.02	bdl	bdl	bdl
F	bdl	bdl	0.11	0.11	0.17	0.21	0.20	0.08	0.08	0.11
Cl	bdl	bdl	0.07	0.04	bdl	0.01	bdl	bdl	bdl	bdl
O=-F	—	—	-0.05	-0.05	-0.07	-0.09	-0.08	-0.03	-0.03	-0.05
O=-Cl	—	—	-0.02	-0.01	—	-0.00	—	—	—	—
H_2O*	—	—	5.72	5.75	1.83	1.82	1.84	—	—	—
∑ oxide	98.30	99.24	100.12	100.45	99.13	99.68	99.79	93.76	97.52	98.92
Si	6.002	5.984	3.577	3.568	9.118	9.353	9.307	12.743	11.976	11.914

Al	0.051	0.062	0.053	0.062	1.502	0.980	1.020	0.519	0.462	0.763
Y	—	—	—	—	—	—	—	0.473	—	—
Be	2.000	2.000	2.370	2.370	2.380	2.667	2.673	2.000	2.000	2.000
Fe	—	—	0.018	0.014	—	0.004	0.005	—	—	—
Mn	—	—	—	—	—	0.007	0.005	—	—	—
Mg	—	—	—	0.018	—	0.002	—	—	—	—
Sr	0.013	—	—	—	—	—	—	—	—	—
Ba	—	—	—	—	—	0.002	0.001	—	—	—
Cs	—	—	—	—	—	—	0.002	—	—	—
Rb	—	0.011	—	—	—	—	—	—	—	—
Ca	0.025	0.013	2.796	2.790	4.128	4.093	4.128	1.542	2.075	2.068
Na	1.746	1.820	0.166	0.158	—	0.076	0.065	0.111	0.220	0.109
K	0.020	0.021	—	—	—	0.006	—	1.085	1.267	1.146
P	—	—	—	—	—	0.002	0.003	—	—	—
∑ cat	9.857	9.911	8.980	8.980	17.128	17.192	17.210	18.473	18.000	18.000
F	—	—	0.027	0.027	0.084	0.102	0.098	0.047	0.042	0.057
Cl	—	—	0.009	0.005	—	0.002	—	—	—	—
H	—	—	2.964	2.968	1.916	1.897	1.902	—	—	—
O_{tot}	15.000	15.000	13.964	13.968	27.916	27.897	27.902	31.091	29.443	29.639

Note: * determined by stoichiometry; bdl = below detection limit
epididymite - contents on a basis of 15 O and Be = 2
hydroxylgugiaite - contents on a basis of 14 anions
bavenite - contents on a basis of 28 anions and Be = 13 - (Si + Al)
milarite - contents on a basis of 18 cations = ∑ (Na, Si, Al, Mg, Ca, K, Be) and Be = 2